NACA

RESEARCH MEMORANDUM

COMPARISON OF SEVERAL METHODS OF CYCLIC DE-ICING OF A GAS-HEATED AIRFOIL

By Vernon H. Gray and Dean T. Bowden

Lewis Flight Propulsion Laboratory
Cleveland, Ohio

NATIONAL ADVISORY COMMITTEE
FOR AERONAUTICS

WASHINGTON

June 22, 1953

NATIONAL ADVISORY COMMITTEE FOR AERONAUTICS

RESEARCH MEMORANDUM

COMPARISON OF SEVERAL METHODS OF CYCLIC DE-ICING OF A GAS-HEATED AIRFOIL

By Vernon H. Gray and Dean T. Bowden

SUMMARY

Several methods of cyclic de-icing of a gas-heated airfoil were investigated to determine ice-removal characteristics and heating requirements. The cyclic de-icing system with a spanwise ice-free parting strip in the stagnation region and a constant-temperature gas-supply duct gave the quickest and most reliable ice removal. Heating requirements for the several methods of cyclic de-icing are compared, and the savings over continuous ice prevention are shown. Data are presented to show the relation of surface temperature, rate of surface heating, and heating time to the removal of ice.

INTRODUCTION

The advent of high-speed, all-weather, jet-powered aircraft has emphasized the need for ice-protection systems that are light-weight, dependable, and automatic and that impose the least possible penalty on over-all aircraft performance. Anti-icing systems that evaporate all the impinging water cause practically no increase in drag but, at high speeds, require large rates of surface heating (ref. 1). These large heating requirements in an electric system call for a large generating capacity, which involves excessive weight; in a hot-gas system large flows of heated air are required, resulting in excessive thrust losses when the air is taken from the jet-engine compressor.

The large heating requirements associated with continuous anti-icing can be greatly reduced by the use of a cyclic de-icing system, wherein only one spanwise segment of an airfoil is heated and de-iced at any given time. Intermittent heating and shedding of ice successively from many such segments in repeated cycles will permit a given heat flow to de-ice many times as much area as would be continuously anti-iced by the same flow. Consequently, a large reduction in the over-all heating requirement for an airfoil is realized.

Cyclic de-icing may be accomplished by using either electric or hot-gas heat sources. A typical electric cyclic de-icing system is described

in reference 2. Heating requirements and resultant penalties for an aircraft with this type of ice-protection system are given in reference 1. Recently, efforts have been directed toward the development of hot-gas cyclic de-icing systems. The principal advantages of hot-gas cyclic de-icing are: The heat supply is readily available at the jet engines; the surface heating channels may be constructed integrally with the airfoil structure to permit a low weight-increase factor; and the operation of hot-gas systems is basically reliable, so that low maintenance costs result. The first experimental investigation of cyclic de-icing with hot gas is reported in reference 3, in which successful de-icing was accomplished with considerable savings of heat over continuous anti-icing.

The effect of a hot-gas cyclic de-icing system on aircraft performance has not been completely evaluated at present. However, the drag increases associated with hot-gas cyclic de-icing are presented in reference 4. Drag data obtained for an 8-foot-chord NACA 65_1-212 airfoil indicate that only moderate airfoil drag increases are to be expected from runback icing caused by cyclic ice removal and that after ice removal the drag returns almost to the bare airfoil drag. Only in severe icing conditions with high rates of water interception does the drag increase during the icing period exceed 15 percent.

This investigation presents a comparison of heat requirements and ice-removal characteristics for several methods of cyclic de-icing with hot gas. The de-icing systems investigated differed principally with regard to the means of obtaining elevated gas temperatures at the surfaces to be de-iced and in regard to the use of ice-free parting strips in the stagnation region to facilitate ice removal. Because of the present lack of fundamental knowledge on cyclic de-icing processes, extensive data on heating rates, surface temperatures, and ice-removal times for various surface locations are presented to provide a basis for future analytical treatments. The investigation was made in the NACA Lewis icing research tunnel over a wide range of icing and operating conditions.

APPARATUS AND INSTRUMENTATION

Each hot-gas cyclic de-icing system investigated was installed in an NACA 65_1-212 airfoil of 8-foot chord and 6-foot span (fig. 1). This airfoil was also used in the investigation of reference 3, some of the results of which are included in this study for purposes of comparison. Of the various cyclic de-icing systems studied, three systems which were thoroughly investigated will be described in subsequent sections and identified as heating systems A, B, and C.

Heating System A

In this report, the heating system utilized in reference 3 will be termed heating system A. The construction details are shown in figure 2 and table I. The heatable forward section of the model extends from 0 to 12 percent of chord and consists of three spanwise segments which may be independently heated. The center segment is 3 feet in span and contains most of the instrumentation.

The gas-supply duct (fig. 2(a)) is a relatively small thick-wall double-passage aluminum duct mounted inside the airfoil near the leading edge but isolated from all metallic airfoil structure and insulated to reduce convective heat losses. The hot gas flows spanwise in the front passage of the double duct and reverses direction at the end of the span to return in the rear duct passage. Along the rear passage, throttling valves are located, one at each intermittently heated segment. A fourth valve is provided at the exit end of the rear passage to represent all the additional segments that would be used in an actual long-span wing.

An aluminum fin is used to conduct heat from the double-passage duct to the stagnation region to provide an ice-free parting strip. The spanwise fin is approximately 1/16 inch thick and $3\frac{1}{2}$ inches long and is made in two parts screwed together at a slip joint for convenience in model assembly and to allow for thermal expansion. Chordwise parting strips between the center and end segments are provided for in a manner similar to the spanwise parting strip, except that the slip joint is omitted. Dimensions of the parting-strip fins are given in table I.

The outer skin of the airfoil forward section is made of 0.025-inch-thick aluminum alloy. Strength and rigidity are provided by an inner skin of 0.040-inch-thick aluminum alloy corrugated with a 1-inch spanwise pitch to produce chordwise gas passages of 1/8-inch height.

Entrances to the passages formed by the outer skin and corrugated inner skin are located near the spanwise parting strip on both top and bottom surfaces of the airfoil (fig. 2(b)). The passages extend to approximately 12 percent of chord. After leaving the passages, the gas is permitted to exhaust through the aft regions of the airfoil. Bulkheads at either end of the center segment are insulated to reduce spanwise heat losses during the heat-on period. Asbestos sheeting is used to insulate the corrugated inner skin from the plenum chamber to allow the gas to enter the chordwise passages at maximum temperature.

The poppet-type throttling valves were timed electrically and actuated by means of compressed air.

Heating System B

Heating system B is the same as heating system A (fig. 3(a)) except that none of the parting-strip fins are heated by the supply duct (fig. 3(b)). The parting-strip fins remain riveted to the outer skin of the airfoil but are thermally disconnected from the supply duct by air gaps of at least 0.050-inch thickness.

Heating System C

Heating system C is the same as heating system B, except that it has a nonreturn gas-supply system. For this system the gas enters the rear passage of the supply duct and flows spanwise directly to the throttling valves. No gas flows through the front passage, and the parting-strip fins are thermally disconnected from the supply duct by air gaps as in system B (fig. 3(c)).

Instrumentation

The instrumentation used for the three heating systems is as follows:

(1) Gas-temperature thermocouples and static-pressure tubes in both passages of the supply duct at five spanwise locations

(2) Gas-temperature thermocouples inside the chordwise gas passages at six chordwise and four spanwise points, and at four points in the plenum chambers

(3) Surface-temperature thermocouples at 24 chordwise points on section A-A in the center segment, and at five other spanwise stations

(4) Metal-temperature thermocouples at such points as ribs, spar, supply duct, inner-skin corrugations, and conductive fins at four spanwise stations

(5) Static-pressure taps in the plenum chambers and in the airfoil afterbody.

EXPERIMENTAL CONDITIONS AND TECHNIQUES

The range of conditions covered in the investigation is as follows:

Total air temperature, °F	-11 to 25
Airspeed, mph	180 and 280
Angle of attack, deg	2, 5, and 8
Pressure altitude, ft	1500 to 3500
Liquid-water content, g/cu m	0.3 to 1.2
Mean-effective droplet diameter, microns	8 to 18
Duct-inlet gas temperature, °F	200 to 510
Duct gas-flow rate, lb/hr	110 to 1230
Heat-on period, sec	6 to 48
Heat-off period, min	4 to 10

In order to establish a convenient reference temperature on which to base heat-transfer processes, a datum air temperature was taken as the average unheated-surface temperature of the airfoil forward section. In icing conditions, the datum temperature was determined from thermocouples that were shielded from, or not subject to, the heat of fusion of impinged water. The datum air temperature was found to be essentially equal to the total air temperature for the conditions covered in this investigation.

In order to evaluate and compare the various methods of cyclic de-icing, each method was thoroughly investigated for the following nominal conditions:

Datum air temperature, °F	Liquid-water content, g/cu m	Airspeed, mph
0	0.6	180, 280
20	.8	180, 280

For most of the above conditions, performance of the various systems was investigated at angles of attack of 2°, 5°, and 8°.

In order to determine and compare the minimum heating rates necessary for satisfactory cyclic de-icing of the airfoil forward section for the various heating systems, a visual criterion for marginal performance was adopted. The heating rate and heat-on period were deemed marginal for a particular icing condition when ice was completely removed from both surfaces of the airfoil back to 9 percent of chord (slightly aft of plenum chamber). In addition, parting strips, when provided, were required to remain ice-free.

During the investigation of heating rates required for continuous anti-icing, marginal requirements were established at the heating rate which would completely evaporate all the impinged water, and thereby prevent the occurrence of runback icing anywhere on the airfoil surface.

Photographs of both surfaces of the airfoil forward section were taken throughout the investigation to record the type and extent of

icing, the effectiveness of ice shedding (ice removal), and the amount of residual ice and frozen runback rivulets. Photographs were synchronized with temperature data and observations of ice removal from specific points during the heat-on period.

RESULTS AND DISCUSSION

The results will be presented in two main phases. The first phase concerns the over-all operation and performance of the heated airfoil forward section, wherein the marginal heating rates for the various methods of cyclic de-icing are determined by the visual criterion of ice removal defined in the previous section. In the second phase, temperature data amenable to analysis and extrapolation to other models are obtained. In this phase, the local variations of temperature and ice removal with time are presented without consideration for marginal operation or the effectiveness of de-icing.

Over-All Performance of Cyclic De-Icing Systems

Typical ice formations with marginal de-icing. - Ice formations characteristic of marginal de-icing in various atmospheric and operating conditions are shown in figure 4 by photographs of the airfoil forward section before and after the heat-on periods. The difficulty and possible variance in establishing consistent marginal heating conditions are apparent from these photographs. Varying amounts of residual and runback icing can be seen in the photographs taken after the marginal heat-on periods. Negligible runback icing is shown in figure 4(a). In figure 4(b) runback deposits have begun to collect directly impinging droplets and are growing forward and outward. The deposits aft of the heated forward section are caused by impingement upon frost particles. The airfoil invariably frosted as soon as water sprays began, probably because of air-stream turbulence and supersaturation of the tunnel air, which is not the usual case in flight. Primary impingement icing on the upper surface was always completely removed, as shown typically in figure 4(c). Runback icing on the upper surface consisted of thin streaks of ice starting about 9 inches back from the leading edge. These runback streaks did not grow materially, because they shed sporadically during subsequent heat-on periods.

Effect of angle of attack, liquid-water content, and icing period on heating requirements. - As reported in reference 3, the airfoil angle of attack, the liquid-water content, and the icing period had relatively small effects on marginal heat requirements. An increase in these three variables tended to increase slightly the required heating rate or heat-on period. These trends result partly from the criterion adopted for determining marginal requirements. At 9 percent of chord on the lower surface, aerodynamic forces are not significantly changed by varying the angle of attack; of more importance is the aft limit of impingement. At higher angles of attack, ice collects farther aft on the lower surface.

Because of the front-to-rear gas flow in the chordwise gas passages, above-freezing surface temperatures appear progressively rearward with time during the heating period. Consequently, longer heat-on periods are necessary at the higher angles of attack to cause removal of the rearmost ice formations. A similar increased heat-on period was found necessary with an increase in the liquid-water content, because an increase in the spray-cloud liquid-water content in the tunnel is associated with an increase in the cloud droplet size, which results in impingement further aft on the airfoil surface.

The combined effect of angle of attack and liquid-water content upon impingement is shown in figures 4(a) and 4(b). At an angle of attack of 2° and a liquid-water content of 0.4 gram per cubic meter (fig. 4(a)), impingement extended less than 2 inches aft of the spanwise parting strip on the lower surface; at an angle of attack of 8° and a liquid-water content of 0.8 gram per cubic meter, the impingement extended more than 8 inches behind the spanwise parting strip (fig. 4(b)). An example of runback icing caused by a high liquid-water content and a high angle of attack at a high datum air temperature is shown in figure 4(e). Sizable glaze-ice deposits are seen at the rear end of the heated section. These deposits shed sporadically as their size and the drag forces on them increased.

An increase in the icing period also requires a slight increase in the heat-on period, probably because of increased time for cooling of the model interior, increased ice thickness, and reduced tendency of ice that has been under-melted to break away from anchoring points at local cold areas during the heating period. The increase in ice thickness as a result of increasing the icing period from 6 to 8 minutes can be seen by comparing figure 4(c) with figure 4(d).

Theoretically, a decrease in the heating requirement might be expected with increasing liquid-water content because of the associated increased release of heat of fusion and consequent increased surface temperature prior to heating. However, this effect is almost lost to the de-icing system because of the insulating effect of the ice layer, the moderate chordwise extent of heavy impingement, and the high conductivity of the airfoil structure which conducts the heat of fusion away from the impingement zone. The effect of heat of fusion on surface temperature is illustrated in figure 5. The unheated-surface temperatures of the forward section are shown in dry-air flow and in icing conditions. After icing begins, the surface temperatures rise to a maximum in approximately 1 minute (fig. 5(b)). The greatest rise due to the release of heat of fusion (8° F) occurred at the stagnation point. On an insulated surface this rise would have been nearly three times as much (based on unpublished NACA data obtained with a lucite cylinder in a comparable icing condition). The average surface temperature, however, rose only 3° F above the dry-air average surface temperature after 1 minute of icing, and only 2° F above the dry-air level after 4 minutes of icing. The local

surface temperatures deviated from the average by a maximum of $\pm 5^{\circ}$ F after 4 minutes of icing, with the lower surface averaging 6° F warmer than the upper surface. It is interesting to note also that the average surface temperature of the forward section was $3\frac{1}{2}^{\circ}$ F below the total air temperature in dry-air flow and only $\frac{1}{2}^{\circ}$ to $1\frac{1}{2}^{\circ}$ F below the total temperature in icing conditions.

Heating rates required for marginal de-icing performance. - The heat-on period required for marginal ice removal is shown in figure 6 for a range of icing conditions. During the heat-on period, the rate of heat flow per foot of span at the throttling valve $wc_p(t_{g,v} - t_d)$ is plotted as a function of the heat-on period for heating systems A, B, and C. (Symbols are defined in the appendix.) In the case of heating system C, which has a nonreturn gas flow (fig. 6(c)), the gas flows through relatively cold ducting and the gas temperature increases throughout the heating period; for this case the gas temperature at the throttling valve $t_{g,v}$ is taken as the average during the heat-on period.

For all cases shown, the required heating rate increases with a decrease in the heat-on period. This increase in heating rate is particularly marked for heat-on periods of less than 10 seconds. Heating system B, however, requires approximately a 30-percent increase in the heating rate over that for system A for the same heat-on period, and heating system C requires approximately a 40 percent higher heating rate than system A. For a constant heating rate, however, the change in heat-on period between heating systems is even greater. The average of the changes for all icing conditions investigated shows that heating systems B and C require approximately 50 and 85 percent longer heat-on periods, respectively, than does system A, for equivalent heating rates.

In order to show the effect of datum air temperature on the heating rate for constant values of heat-on period, the data of figure 6 are cross-plotted in figure 7. The air temperature is seen to have a very large effect upon the heating rate, requiring 50 to 100 percent more heat flow at 0° F than at 20° F. The most rapid increase in the required heating rate as the air temperature decreases occurs near 32° F; at colder air temperatures, the heating rate increases less rapidly.

The effect of airspeed on the heating rates required for marginal de-icing is shown in figure 8 and was found to be small. An increase in airspeed from 180 to 280 miles per hour required approximately a 10-percent increase in the heating rate for systems A and B and approximately 20 percent for system C, with other factors remaining constant. Also shown in figure 8 for purposes of comparison are the heating rates required for continuous anti-icing as defined in EXPERIMENTAL CONDITIONS AND TECHNIQUES. It is interesting to note that, although the short-duration heating rate required to de-ice the model is generally higher

than that required to continually anti-ice it, the velocity effect is such that the two quantities are of the same order of magnitude at the higher airspeeds shown. The over-all heat savings of cyclic de-icing as compared with continuous anti-icing will be shown later.

Spanwise reduction in gas temperature. - In order to assess the total heating requirements of the various heating systems, the spanwise gas-temperature drop in the supply duct must be considered as well as the heating rate at the valve during the heat-on period. The spanwise gas-temperature reduction may result from heat transferred through the parting-strip fins (when provided) and from duct losses by conduction, convection, and radiation. For heating systems A and B, which utilize the return-flow gas circuit, the gas temperature decreased progressively in the front passage of the duct and remained essentially constant in the rear or return passage. Accordingly, the gas-temperature drop along the front passage of the duct was taken to represent the effect of span on gas temperature. For heating system C, however, the effect of span on gas temperature could not be determined from the transient data involved.

In figure 9, the decrement of supply-duct gas temperature per foot of span divided by the difference between mean gas temperature and datum air temperature is plotted as a function of gas flow for all the conditions investigated. For cyclic operation of the heating system, the spanwise gas-temperature drop during the heat-off period is shown in figure 9(a). Heating system B, with no parting strips, has approximately two-thirds of the spanwise temperature drop of system A. Data were also taken with the chordwise parting strips removed from system A and with improved sealing at the bulkheads between the spanwise segments. These data fall midway between the curves for systems A and B. A slight trend with respect to air velocity is evident in the data but is not described by separate curves. The scatter of the data in figure 9(a) results from the variety of conditions investigated and the small temperature changes per foot of span. With continuous heating of the forward section (fig. 9(b)), however, the velocity effect is more pronounced and is shown by separate curves. The data fall below those for cyclic operation and show no separation with heating system employed.

Equivalent-continuous heating requirement. - The total heat requirement per foot of span for marginal icing protection is obtained by combining the heating rate at the valve (fig. 6) with the spanwise gas-temperature drop in the supply duct (fig. 9). (These two quantities were not combined in ref. 3.) Because the spanwise temperature loss in the duct is a continuous function and the heat flow through a valve is intermittent, an equivalent-continuous heating requirement is derived for the intermittent process. The portion of time that a valve is open is the ratio of the heat-on period to the total cycle time. The product of this ratio and the instantaneous heat flow through a valve equals the equivalent-continuous heating rate at the valve. Adding to this the continuous heat dissipation from the spanwise supply duct yields the system

(or total) equivalent-continuous heating rate. This function has the physical significance of being the heat-source requirement for an airfoil composed of a number of segments equal to the cycle ratio of each segment. The cycle ratio R is the total cycle time divided by the heat-on period.

With heating system C, the spanwise gas flow in the supply duct is discontinuous and the duration of flow varies with the spanwise location of the segments. However, for the 4-minute heat-off period usually employed in this investigation, the heat dissipated from the supply duct when maintained at an elevated temperature was approximately the same as the heat absorbed by the duct when gas flow was resumed after a cooling period with no gas flow in the duct. For this reason it was assumed that the heat dissipation from the spanwise supply duct for system C, regardless of spanwise location of the segment, was equivalent to the steady-state heat loss of system B for comparable conditions.

The total equivalent-continuous heating requirement per foot of span for the three heating systems is shown in figures 10(a) to (c) as a function of the cycle ratio. The equivalent-continuous heating rates required for the three heating systems do not differ as much as the heating rates required for de-icing only, as shown in figure 6. Because the parting-strip heat dissipation of system A is continuous, it partially offsets the longer heat-on periods (fig. 6) required for systems B and C. The total equivalent-continuous heat requirement of system C is from 10 to 50 percent greater than that for system A for the same cycle ratios, with system B only slightly greater than system A.

For cycle ratios greater than 12, it can be seen from figure 10 that a heat-source capacity of 3000 Btu per hour per foot of span for heating systems A and B and 3250 Btu per hour per foot of span for system C will provide de-icing protection in the following severe condition: airspeed, 280 miles per hour; datum air temperature, 0° F (approximately -9° F static temperature); liquid-water content, 0.6 gram per cubic meter. Cyclic operation at larger cycle ratios than those shown in figure 10 will result in little additional saving in equivalent-continuous heat requirements. It should be remembered that the data presented are for an icing (heat-off) period of approximately 4 minutes. If the icing period had been doubled, the heating rate during the heat-on period would have been only slightly increased, but the cycle ratios would have been nearly doubled and the heat-source requirements would have been considerably decreased. The choice of icing period depends upon the amount of ice to be collected, and it is limited between the time required for the surface to cool below the freezing level and the time in icing that the aircraft may tolerate in terms of aerodynamic penalties.

In figures 10(a) to (c) air temperature is seen to have a large influence on the heat-source requirement, exhibiting the same trends as

in figures 6 and 7. The change in air velocity from 280 to 180 miles per hour reduces the equivalent-continuous heating requirements by an average of 15 percent.

Some of the data of figure 10(a) are replotted in figure 10(d) to effect a comparison with the heating requirements for continuous anti-icing of the forward section (cycle ratio = 1). The continuous heating requirements are between 4 and 10 times higher than the cyclic de-icing heat requirements at cycle ratios between 10 and 20. The greater savings with cyclic de-icing occur at the higher air velocities and higher liquid-water contents. These conditions result in a higher rate of water catch with a direct increase in the heat required for evaporation, whereas only a slight increase in heat flow is required to de-ice the airfoil (fig. 8).

With continuous anti-icing the upper airfoil surface was most critical, becoming marginal with heating rates 40 to 80 percent greater than those required to maintain the lower surface marginal. This effect is probably explained by the impingement characteristics of the airfoil at the angles of attack investigated. Rivulet flow (which is hard to evaporate) is promoted over the upper surface by the heavy accumulation of impingement between the stagnation point and the zero chord point and by the strong air forces which blow this water over the upper surface of the airfoil. However, it should be noted that the heating requirements for continuous anti-icing could be greatly reduced if small amounts of streamlined runback ice formations were tolerated on the upper surface aft of the critical leading-edge radius region.

Although the equivalent-continuous heating requirement is a direct measure of the heat-source requirement, it does not completely describe the heat-transfer process, because it contains terms of both gas flow and gas temperature, which usually do not contribute alike to the heat-transfer process. Some of the scatter of the data points in figures 6 to 10 results from the use of $wc_p\Delta t$ as a heating parameter. The independent effects of gas flow and gas temperature are shown in figure 11, in which gas flow and temperature were varied separately and the heat-on periods for marginal de-icing performance were determined. The equivalent-continuous heating requirement is shown to decrease with an increase in the gas flow for system A (fig. 11(a)), whereas heating systems B and C show small and zero decrease, respectively, with increased gas flow. When gas temperature is increased (fig. 11(b)), a slight decrease in heating requirement occurs with systems A and B, whereas a slight increase in heating requirement is shown for system C. Heating system C has no preheating of gas-supply passages, and the increased thermal lag may explain the greater heat requirements at higher gas temperatures. Generally, a given percentage increase in the gas flow permits a greater reduction in the heat-source requirement than a comparable increase in the gas temperature.

Parting-strip characteristics. - Data were obtained on the temperature pattern associated with the spanwise parting strip used in system A. From these data the heat-flow rate through the conductive fin and the ice-free width of the parting strip may be determined. A typical temperature pattern is shown in figure 12, in which distances are measured along the heat paths from the juncture of the conductive fin and the external skin. These temperatures were taken after 4 minutes of icing and before cylic removal. The temperature drop between the gas in the duct and the duct wall was small, representing approximately 20 percent of the total drop between gas and peak surface temperature. The temperature drop across the slip joint was approximately 35 percent of the gas-to-surface temperature differential. Without a slip joint, the same heat flow to the parting strip would be maintained with a thinner or longer conductive fin than was used herein. The fin length and thickness are of importance in transmitting the proper amount of heat flow for establishing a narrow parting strip.

The surface-temperature pattern reveals the heating effectiveness in the parting strip. The surface temperature should return quickly to the datum level on both sides of the parting strip to minimize heat losses by conduction along the surface. Such is the case on the upper-surface side of the parting strip, but the lower-surface temperature falls much more gradually. The arrows at approximately 1/2 inch from the center of the parting strip (fig. 12) indicate the start of the corrugated inner-skin passages. The added thickness and conductivity of the double-skin construction require a larger distance for the surface temperature to return to datum.

The width of the parting strip that is above 32° F prior to the heat-on period may be determined from the surface-temperature pattern (fig. 12), and it was found to be conveniently expressible as a function of the temperature ratio $\frac{t_{s,max} - 32}{t_{s,max} - t_d}$ shown in figure 13 for all conditions investigated. The parting-strip width is well defined by the temperature data; however, the visual width may be smaller than that of figure 13 because of ice building forward or greater because of warm water running back beyond the line where the surface temperature is 32° F.

The quantity of heat flow to the outer skin passing through the fin is measured by two thermocouples in the fin at a known distance apart. The temperature gradient between the couples (fig. 12) together with the fin cross section and conductivity is used to calculate the total heat flow through the fin. The heat flow through the fin is shown in figure 14 as a linear function of $t_{s,max} - t_d$. The line for an airspeed of 180 miles per hour is interpolated from data not directly applicable to this figure. Figures 13 and 14 may be used together as follows: If, for

example, a parting-strip width of 1 inch is desired, a temperature ratio of 0.45 is required (fig. 13). From the relation $\frac{t_{s,max} - 32}{t_{s,max} - t_d} = 0.45$ and a datum air temperature of 0° F, a required $t_{s,max}$ of 58° F is obtained. At an airspeed of 180 miles per hour the heat flow needed to produce this maximum parting-strip temperature is 280 Btu per hour per foot span (fig. 14), which is an average heating rate in the parting strip of 6.8 watts per square inch. For the same conditions, the electrically heated parting strip of reference 2 required an external surface heat flow of 6.6 watts per square inch.

Variations in mode of heating. - Several variations in the mode of heating were investigated briefly. One variation was the use of a secondary cycling procedure in which submarginal operation of the heating system was employed for several successive cycles followed by a cycle with above-marginal heating to reduce the amount of lower airfoil surface runback and residual icing. In this manner, the runback icing from the submarginal cycles was deposited upon the rear portions of the heated area and was removed during the above-marginal cycle, thereby considerably reducing the amount of permanent runback icing. An above-marginal cycle may be achieved by increasing either the gas flow, the gas temperature, or the heat-on period. In this study, with heating system A, the heat-on period was increased every fourth cycle; the heat-off period was proportionately increased to maintain the same cycle ratio. A comparison of the runback icing after three submarginal (short) cycles and a fourth (long) cycle is shown in figure 15. Most of the accumulation of runback ice from the three short cycles is removed by the long cycle, leaving very little residual icing after 2 hours and 49 minutes of operation. Improved performance would probably result if the double-skin construction extended a few inches farther aft of the plenum-chamber partition (fig. 2(b)) to ensure that the runback would freeze on the heatable area and not build forward from unheated areas.

Another variation in the heating method was investigated to determine the response of heating system A from a cold start in icing conditions. The cold model was allowed to collect ice for 4 minutes, and then a cyclic heating routine was begun. During the preliminary 4 minutes of icing on the cold model, gas temperatures and flow rates corresponding to standard marginal operation of the system were maintained in a supply pipe up to a point approximately 5 feet from the model inlet. When heat flow to the center segment began, the gas therefore traveled through 5 feet of cold piping plus the double-duct return-flow circuit within the model. The first heating period of the cold and iced model removed practically no ice; whereas the second heating period, after 4 minutes of duct and parting-strip heating, removed the 8-minute growth of ice as completely as in the standard cyclic operations. In order to determine the heat-up time more closely, the gas flow was directed through the double-duct

circuit for varying lengths of time before the first period of heating to the double-skin areas was begun. After 2 minutes of duct heating following the preliminary icing period of 4 minutes, a heating period corresponding to standard marginal operation removed the ice formations practically as well as in standard operation. However, after only 1 minute of duct preheating, ice removal was erratic and incomplete, as shown in figure 16.

The gas temperature at the center throttling valve is shown in figure 17 for three flow conditions as a function of time after the start of hot-gas flow through the double duct of a cold and iced model in the following icing conditions: airspeed, 280 miles per hour; datum air temperature, 0° F; liquid-water content, 0.6 gram per cubic meter; angle of attack, 5°; heating system A. For the two curves of higher gas-flow rates in figure 17 (805 and 710 lb/hr), the gas temperature after 1 minute of flow reached approximately 70 percent of the ultimate temperature rise, and after 2 minutes was about 90 percent of the ultimate rise. Considering the observations of ice removal previously noted, the de-icing ability of a cyclic system from a cold and iced start is apparently entirely a function of the time required to heat the duct work and permit delivery of sufficiently hot gas to the plenum chambers.

The temperature curves for the duct wall at the center valve are shown in figure 18 for heating systems A and C and are compared with the curve of the gas-temperature rise. For heating system A, the temperature rise of the duct generally follows the curve of the gas-temperature rise except at a slightly lower temperature level. However, for heating system C, the duct cooling curve (after termination of gas flow) was much less steep than the heating curve. For the heating cycle shown, the duct heating time was only one-tenth the time required to cool the duct between the same temperature limits. The performance of heating system C is made possible by the slow rate of cooling of the duct. If the duct should cool to ambient temperature between cycles, heat-on periods of at least 1 minute are indicated for a one-directional flow system, such as in system C.

A few tests were made with the asbestos sheeting removed from the plenum chamber along the lower-surface corrugated inner skin. The differences observed indicate that the thin insulation sheeting has a large influence on the distribution of heat flow to the outer skin. With the insulation installed and with use of heating system A, ice shedding occurs first at the leading edge and then progresses rearward. The reverse is generally true when the insulation is removed, the first shedding occurring just forward of the plenum-chamber partition. This action indicates that heat transfer directly through the double skin from the plenum chamber is a large factor without insulation. Furthermore, slightly less heating along the upper surface is evident when the lower-surface insulation is removed. Even though the heat-on period required for marginal de-icing as defined herein is approximately the same with or without this insulation, it was evident that, for more reliable ice removal from the leading

edge and along the top surface, insulation should be provided to confine the release of heat primarily to the passage of gas through the double skin.

A variation of heating system A, in which the chordwise parting strips were thermally disconnected and the spanwise parting strip was retained, was also investigated. Very little change in the ice-removal performance from that of system A was noted, and a small reduction in heat requirements resulted (fig. 9). When the heating rate was otherwise adequate for the conditions investigated, the ice formations which bridged across from adjacent unheated segments would readily break away. Possibly with thicker ice caps and at very low angles of attack, difficulty might arise because of ice-bridging. In this case, chordwise parting strips of lesser extent than in system A would be beneficial, as mentioned in reference 3.

A final variation was investigated in which the gas flow through each passage of the supply duct was made independent of the other. In order to accomplish this variation, the flow in the front duct passage was allowed to exhaust at the end of the airfoil span and the rear duct passage was sealed off at that point. Flow in the rear passage entered the model through the normal outlet pipe (fig. 2). In this study, the spanwise parting-strip fin was connected to the duct as in system A, and the gas flow was supplied continuously to the front duct passage and cyclically to the rear passage. Cyclic de-icing performance equivalent to that of heating system A was achieved with the front-passage gas flow reduced to less than half of the normal flow for system A, while the mean gas temperature and other conditions remained the same. The spanwise gas-temperature drop in the front passage, however, varied inversely with the gas flow, as shown in figure 9.

The cyclic de-icing performance of the flow in the rear passage is greatly affected by the duct-wall temperature which, in turn, is determined by the gas temperature in the front passage. For the same flow conditions in the rear passage, an increase in heat-on period required for marginal de-icing is shown in figure 19 for a decrease in the gas temperature in the front duct passage. At the highest gas-temperature point (450° F), the heat-on period approaches that of system A; while at the lowest gas-temperature point (195° F), the performance is approximately that of system C. Extending the curve down to a temperature level of 0° F would yield a heating time between 1 and 2 minutes, which corresponds with data previously shown for cold starts.

The heat-storage capacity of the duct and fin influenced the de-icing performance. With no flow through the front duct passage, the heat left in the duct assembly after a cyclic heating period was almost sufficient to maintain an ice-free parting strip for a 4-minute icing period at a datum air temperature of 0° F and an airspeed of 280 miles per hour, as

illustrated in figure 20. Where the parting strip was not ice-free after 4 minutes of icing, only a thin layer of transparent ice extended across it. This result suggests the possibility of a spanwise fin of sufficient mass (possibly a structural member) to create an ice-free parting strip without necessarily being connected to the supply duct. The fin would absorb heat from the hot gas in the plenum chamber during the heat-on periods and gradually dissipate it during the icing periods.

Comments on operation of airfoil model. - The gas-heated airfoil model performed reliably for more than 500 hours of operation in the icing research tunnel. No buckling or wrinkling of the airfoil structure or skin occurred as a result of thermal strains. The front-spar temperature remained within 10° F of the datum air temperature throughout the studies. The maximum structure temperature occurred along the inside flange of a noninsulated rib in the forward section. The highest maximum temperature recorded at this point during marginal operation of the various de-icing systems did not exceed 250° F; this peak temperature would have been considerably lower if insulation had been used to cover the ribs.

Local Variations of Temperature and Ice Removal with Time

In the second phase of this investigation, the local variations of temperature and ice removal with time are presented to establish the mechanisms by which thermal de-icing occurs. The shedding of ice at specific locations is studied without consideration for the over-all effectiveness of de-icing; hence, no marginal heating requirements or heat-on periods are specified.

Variation of surface temperature with heating time. - By continuously recording the temperature of each surface thermocouple and simultaneously observing the surface, a close correlation was obtained between surface temperatures and shedding of ice. Several illustrative surface temperature-time curves are shown in figure 21. The curves exhibit considerable variety in shape and mode of ice removal. The curves sometimes have a noticeable inflection at 32° F (see curves a, b, and c). At the point of ice removal the curves frequently have an inflection or discontinuity. High rates of surface heating tend to reduce the apparent disturbances in surface temperature caused by external processes. The process having the greatest effect on the surface temperature curve is that of water and melting ice flowing along the surface. The normal rising tendency of the temperature curve is delayed and sometimes reversed by water flows from melted ice (see curves b, c, and d). Frequently an ice cap will extend over this running water, and, when the ice sheds, the water immediately blows away or forms tiny rivulets and the surface temperature then climbs rapidly (see curve c). Sometimes, when the water finds another path under the ice, the surface becomes dry and a rapid

surface-temperature increase prior to shedding occurs (see curve d). During the cooling portion of the cycle near 32° F, a delay in the return of surface temperature to datum, caused by release of latent heat of fusion during the refreezing process, is sometimes evident. The slight rise in surface temperature just prior to the start of heating for the thermocouples near the leading edge occurred because of leakage into the plenum chamber from an adjacent spanwise segment that was undergoing a heating period. Similarly, a slight delay in the cooling curve immediately after termination of heating is sometimes evident during the heating period of the other adjacent segment (see curve a).

The temperature at which shedding of ice occurred varied from 32° F to over 100° F. Although repeated cycles in the same runs reproduced the same data, the results from different sets of conditions were varied and unpredictable. These varied results are especially true for the surface temperature at the time of ice removal. The random variation in ice-removal surface temperature appeared to be caused by local variations in the rate of temperature rise and local changes in the aerodynamic forces. These factors influence the extent of ice-bridging during the heating periods.

Grouping the temperature curves of adjacent thermocouples together permits a simultaneous study of the shedding process over both airfoil surfaces. In figure 22, curves from four upper-surface thermocouples are shown with melting and shedding times denoted. These curves were obtained from successive cycles in the same set of conditions but may be considered concurrent, because the repeatability between cycles was quite good. The ice formation for figure 22 extended only over the two thermocouples nearest the leading edge. Melting under this ice cap affected thermocouples further aft, as can be seen by depressions in the temperature curves when water flows over the thermocouples. For a different icing condition, temperature curves for the lower-surface thermocouples are shown in figure 23. At the instant ice shed from each thermocouple, the lower surface was photographed. These photographs are shown in figure 24. A definite tendency toward a rear-to-front shedding process is shown in figures 23 and 24. This tendency is characteristic of heating system C. The two thermocouple locations nearest the leading edge were the last to shed ice, although their initial rates of temperature rise were the highest. Both of these thermocouples were under the thick leading-edge ice cap, but their temperature curves were different because of the local water flow under the ice cap. The photographs in figure 24 also show the unevenness in heating over the surface area, which is evidenced by the first de-icing along rivet rows and rib locations.

In conjunction with the uneven heat release to the surface during the heating period, data were obtained to determine the variations in the temperature rise about a typical chordwise double-skin passage. An example is shown in figure 25 for a position on the lower surface 4.9 inches

from zero chord. The surface temperature at the contact point between the inner and outer skins (curve q) reached a slightly higher peak temperature than the surface point on the center line of the passage (curve r) because of conduction in the inner skin. The inner-skin thermocouple at the passage center line (curve p) measured the highest metal temperature of the three. The gas temperature in the plenum chamber (curve n) is also of interest. After 15 seconds of heating, the gas temperature in the plenum (approximately 1 in. from the insulation on the inner skin) had risen to only 314° F, as compared with a temperature of 467° F at the valve. The loss of heat to structure is thus seen to be a large item in the cycle. The plenum area after 4 minutes of heat-off was still over 110° F. The gas temperature in the chordwise passages (curve o), on the other hand, rose and dropped very rapidly after the start and end of heating.

A brief study was made to determine the relative importance of ice and water impingement on surface temperatures and ice-shedding characteristics. For comparison, a dry-air heating cycle was made, then a normal icing and de-icing cycle with impingement, and then a normal icing period after which water impingement was terminated just prior to the de-icing or heating period. The results for two leading-edge thermocouples are shown in figure 26. The surface temperature for the dry-air case is higher throughout the cycle than that for normal de-icing with impingement. The de-icing curve with impingement terminated before heating, however, exactly follows the normal de-icing curve to the point of ice removal and then rises quickly to overtake the dry-air curve near the peak temperature value. The cooling portion of the curve is identical to that for dry air. These data indicate that during the de-icing process the surface ice has a large effect on the surface temperature, and the presence or absence of water impingement makes little difference. Elsewhere in the cycle, water impingement depresses the surface temperature considerably below the values for dry air.

Chordwise variation of surface temperature during heating period. - The chordwise variation of surface temperature at several time intervals during the heating period is shown in figures 27 to 29 for heating system A. In addition, the temperatures at which ice was observed to shed are shown. The spanwise parting-strip width is shown by the intersections of the 32° F line with the initial surface-temperature curve. The chordwise surface-temperature distribution shows the effect of the parting-strip-fin heat addition (at 1 in., lower surface), the plenum-chamber-partition heat addition (at 8 to 9 in., lower surface), and the temperature peak near the aft limit of water impingement on the upper surface (approximately 0.4 in.).

In figure 27 three levels of gas flow are shown for one icing condition along with the corresponding gas temperatures in the chordwise passages. The gas-temperature variation in the chordwise passages is

nearly linear in all cases and shows a reasonably good utilization of heat over the forward section. With an increase in the gas-flow rate (at the same inlet-gas temperature), the gas and surface temperatures along the passages rise markedly and ice removal occurs sooner. In figure 28 a low heating rate (low gas temperature and flow) is illustrated with a datum air temperature of 20° F. The surface temperature at the point of ice removal is practically the same for all locations. The effect of angle of attack on surface temperature is shown in figure 29. As the angle is changed from 2° to 8°, water impinges more toward the lower surface and peak temperatures on the lower surface decrease, while the upper surface has the opposite trend. Ice-removal temperatures show no consistent trends with angle of attack.

The chordwise surface-temperature variation during the heating period for heating systems B and C is shown in figures 30 and 31, respectively, for two icing conditions. The temperature distribution is similar to that for system A, except that there is much less heat addition at the parting-strip fin.

Effect of heating rate on time to reach 32° F surface temperature. - The heating time required to reach a surface temperature of 32° F and the ice-shedding time are plotted in figure 32 against chordwise location as a function of heating rate for the three heating systems. In all cases, the time to reach 32° F and the ice-shedding time decrease as the heating rate increases. The ice-shedding time for system A increases toward the rear of the lower surface, whereas for system B it is nearly constant over the lower surface. For system C, however, the ice-shedding time increases toward the leading edge. A tendency for the ice-shedding time to approach the time required to reach 32° F is apparent at the rearward locations. For equivalent heating rates, the shedding time required for the thick ice near the leading edge increases from system A to B to C.

Variation of ice-shedding time. - Although the ice-shedding temperature was a random variable, the ice-shedding time was found to be more regular. The functions affecting the ice-shedding time were found to be heating rate, angle of attack, air temperature, heating system, and location on surface; the effects of air velocity, if any, were not determined. The shedding time is presented against heating rate in figure 33 for the significant functions cited. In addition to the trends previously discussed for figure 32, the variation of ice-shedding time with angle of attack is of interest. At the location 0.4 inch from zero chord (toward the lower surface)(fig. 33(a)), the shedding time is usually lowest at an 8° angle of attack and highest at 2°. The explanation for this result is that the air flow over this location at an 8° angle of attack is toward the upper surface; as the angle of attack is reduced, the stagnation point approaches this location, the local air forces decrease, and the flow angle relative to the surface becomes greater. The other locations shown in figures 33(b) to (d) exhibit opposite trends

with change in angle of attack, because air flow in these cases is toward the lower surface. Near the leading edge, therefore, ice-shedding time is shortened as the local air-flow streamlines approach tangency with the surface and is increased as the flow becomes more normal to the surface. Farther aft on the lower surface (fig. 33(d)), ice-shedding time as a function of heating rate varies little with angle of attack, indicating that the flow direction and force are not greatly affected by change in angle of attack. These results indicate that aerodynamic forces are an important factor in the shedding time for ice formations near the airfoil leading edge. In this connection, the influence of the parting strip of system A in reducing the ice-shedding time over that of system B is clearly shown. Also apparent in figure 33 is the fact that the ice-shedding time for specific points on the surface is generally much less than the marginal heat-on period of figure 6, which was based on complete forward-section ice removal at all three angles of attack.

CONCLUDING REMARKS

Selection of the best method of cyclic de-icing with hot gas cannot be made independent of the aircraft to be protected. The choice of the heating system depends largely on the quantity of hot gas available for de-icing purposes and on the system weight and complexity which may be tolerated. Heating system C, with respect to simplicity and lightness of weight, has considerable merit. However, in order to operate with a low flow of hot gas, a high cycle ratio is required for which, for a given icing period, heating system B or A is preferable because of the shorter heat-on period. At present, heating system A is recommended for most installations because of its reliable and quick shedding of the dangerous leading-edge ice cap and good utilization of heat.

A cyclic de-icing system may be controlled in several different ways, such as (1) using a fixed heating rate and cycle ratio designed to cope with a severe icing condition selected on a calculated-risk basis, (2) using a fixed cycle ratio and a heating rate controlled by ambient-air temperature, (3) regulating the heat-on period by the ambient temperature or by the temperature of a critical point on the heated surface (heat-off period maintained either constant or controlled by icing rate or airfoil drag), or (4) preestablishing several schedules of operation to be selected in flight either manually or automatically on the basis of ambient temperature. A simple and presently adequate scheme of regulation appears to be the following: a fixed cycle ratio equal to the number of segments to be de-iced (avoiding periods of dwell or wasting of heat flow); a fixed inlet-gas temperature (as high as possible); and three schedules of operation consisting of (a) gas flow and heat-on period as required for marginal operation in the most severe icing condition, (b) gas flow lower than in schedule (a) with the same heat-on period, and (c) gas flow of schedule (a) with shorter heat-off (and heat-on) periods. During mild icing conditions, schedule (b) would be used,

while during colder or more severe conditions, schedule (a) would be used. Schedule (c) is for the high rates of ice accretion which nearly always occur with high datum air temperatures and for which shorter heat-on periods will suffice to shed the ice. Such a scheme could be used with any of the heating systems discussed and would still permit incorporation of the secondary cycling plan for removal of runback icing discussed previously in "Variations in mode of heating".

Several possibilities of improvement over the present de-icing protection systems became evident during the tests. They were primarily concerned with the structure of the airfoil. Weight savings and simplicity would result if the double duct were located nearer the leading edge to permit a shorter and thinner conductive fin. Elimination of the spanwise-fin slip joint could be accomplished if the fin were made to resemble a pocket comb, the teeth of which would allow for spanwise expansion of the inner edge with respect to the outer edge (outer-skin juncture). For flight operation the valves and actuators could be made much lighter and simpler. Better insulation throughout was indicated to be advantageous by the large heat losses to the highly conductive structure. A more efficient parting strip would result if the outer-skin metal was of low conductivity so that the product of skin thickness and thermal conductivity would be reduced. The rear region of the chordwise passages could be improved by a forward movement of the plenum-chamber partition and by tapering the gap in the passages so the outlet gap is less than the inlet. These changes would increase the utilization of heat in the gas-flow passages and permit better operation with a secondary cycling procedure for shedding of runback icing.

SUMMARY OF RESULTS

From the present investigation of several methods of cyclic de-icing of a gas-heated airfoil, the following principal results were obtained:

1. For equivalent icing conditions and heating rates, when all ice-free parting strips were removed from a cyclic de-icing system, approximately 50 percent longer heat-on periods were required for marginal ice protection; when parting strips were removed and the return-flow (continuously heated) gas-supply duct was changed to a single-passage gas duct, an increase of approximately 85 percent in the heat-on periods was required. Removal of all parting strips reduced the spanwise drop in supply-gas temperature by approximately one-third.

2. The equivalent-continuous or heat-source requirement for marginal cyclic de-icing was nearly the same for heating systems with or without parting strips. The heat-source requirement was increased from 10 to 50 percent when continuous heating of the gas-supply duct was eliminated.

3. The heat-source requirement for cyclic de-icing was between one-fourth and one-tenth of the comparable heating requirement for continuous anti-icing.

4. The heating time required for ice removal was an inverse function of the heating rate; however, the surface temperature at ice removal appeared to be a random variation between 32° and approximately 100° F. The greatest external effect on the surface temperature during the deicing period was caused by flows of water and melting ice over the surface.

5. Parting strips, insulation, and continuous heating of the gas-supply system were advantageous for quick and reliable shedding of dangerous leading-edge ice caps and good heat utilization.

Lewis Flight Propulsion Laboratory
National Advisory Committee for Aeronautics
Cleveland, Ohio, March 9, 1953

REFERENCES

1. Gelder, Thomas F., Lewis, James P., and Koutz, Stanley L.: Icing Protection for a Turbojet Transport Airplane: Heating Requirements, Methods of Protection, and Performance Penalties. NACA TN 2866, 1953.

2. Lewis, James P., and Bowden, Dean T.: Preliminary Investigation of Cyclic De-Icing of an Airfoil Using an External Electric Heater. NACA RM E51J30, 1952.

3. Gray, V. H., Bowden, D. T., and von Glahn, U.: Preliminary Results of Cyclical De-Icing of a Gas-Heated Airfoil. NACA RM E51J29, 1952.

4. Gray, Vernon H., and von Glahn, Uwe H.: Effect of Ice and Frost Formations on Drag of NACA 65_1-212 Airfoil for Various Modes of Thermal Ice Protection. NACA TN 2962, 1953.

APPENDIX - SYMBOLS

The following symbols are used in this report:

c_p	specific heat of air at constant pressure, 0.24 Btu/(lb)(°F)
L	span, ft
R	cycle ratio, (heat-off period plus heat-on period)/heat-on period
t	temperature, °F
t_d	datum air temperature, °F
t_g	gas temperature in supply duct, °F
$t_{g,m}$	mean gas temperature in supply duct, °F
$t_{g,v}$	gas temperature at throttling valve, °F
$t_{s,max}$	maximum surface temperature in parting strip, °F
W	gas flow in supply duct, lb/hr
w	gas flow per foot span, lb/(hr)(ft span)

TABLE I. - DIMENSIONS OF AIRFOIL MODEL AND HEATING SYSTEM A

Airfoil, NACA series	65_1-212
span, ft	6
chord, ft	8
maximum thickness, in.	11.5
Heated forward section, extent, percent of chord	12
center segment span, ft	3
end segments, span, ft	1.5
Double-skin construction, inner-skin thickness, in.	0.040
outer-skin thickness, in.	0.025
inner-skin corrugations, pitch, in.	1.0
inner-skin passages, height, in.	0.12
inner-skin passages, width, in.	0.70
Spanwise parting strip, lower-surface location, percent of chord	1.0
fin thickness, in.	0.062
fin length, in.	3.5
fin material, aluminum	2S0
Chordwise parting strip, surface extent, top surface, in.	3
bottom surface, in.	6
fin thicknesses, top to bottom surfaces, in.	0.051,0.062,0.062, 0.051,0.040,0.025
fin lengths, top to bottom surfaces, in.	2.7,3.0,2.7,1.7,1.5,1.3
Double-passage duct assembly, center-line location, in. from nose	4.4
spanwise length, ft	5.8
material, aluminum	2S0
wall thickness, in.	0.094
cross-sectional area, front passage, sq in.	1.5
rear passage, sq in.	1.7
valve ports, sq in.	1.1
Plenum chambers, rear partition location, in. from leading edge	8
Asbestos sheeting, thickness, in.	0.030

TABLE II. - CONDITIONS FOR FIGURES 21 to 26

Figure	Curve	Airfoil surface	Thermocouple distance from zero chord, in.	Airspeed, mph	Datum air temperature, °F	Liquid-water content, g/cu m	Angle of attack, deg	Gas flow, lb/(hr) (ft span)	Model-inlet gas temperature, °F	Heating system	*Comments
21	a	Lower	1.9	280	0	0.6	5	320	500	B	
	b		4.9				5	345		B	
	c		.4				2	180		A	
	d		.4				5	265		B	
22	e	Upper	3.4	280	0	0.6	2	180	500	A	
	f		1.7								
	g		1.0								
	h		.2								
23	i	Lower	1.9	280	0	0.6	5	265	500	C	Ice removal by peeling from rear
	j		.4								Ice removal in large piece
	k		6.9								Ice removal followed by sliding ice and water
	l		4.9								
	m		2.9								Ice removal by peeling
25	n	Lower	4.9	280	0	0.6	5	265	500	A	Gas temperature at valve, 467° F
	o		4.9								
	p		4.9								
	q		4.9								
	r		4.9								
26	s	Upper	0.2	180	20	0	5	265	325	A	Dry air
	t		.2			*					Impingement terminated before heating
	u		.2			.8					Normal de-icing with impingement
26	v	Lower	0.4	180	20	0	5	265	325	A	Dry air
	w		.4			*					Impingement terminated before heating
	x		.4			.8					Normal de-icing with impingement

Figure 1. - Installation of airfoil model in 6- by 9-foot test section of icing research tunnel.

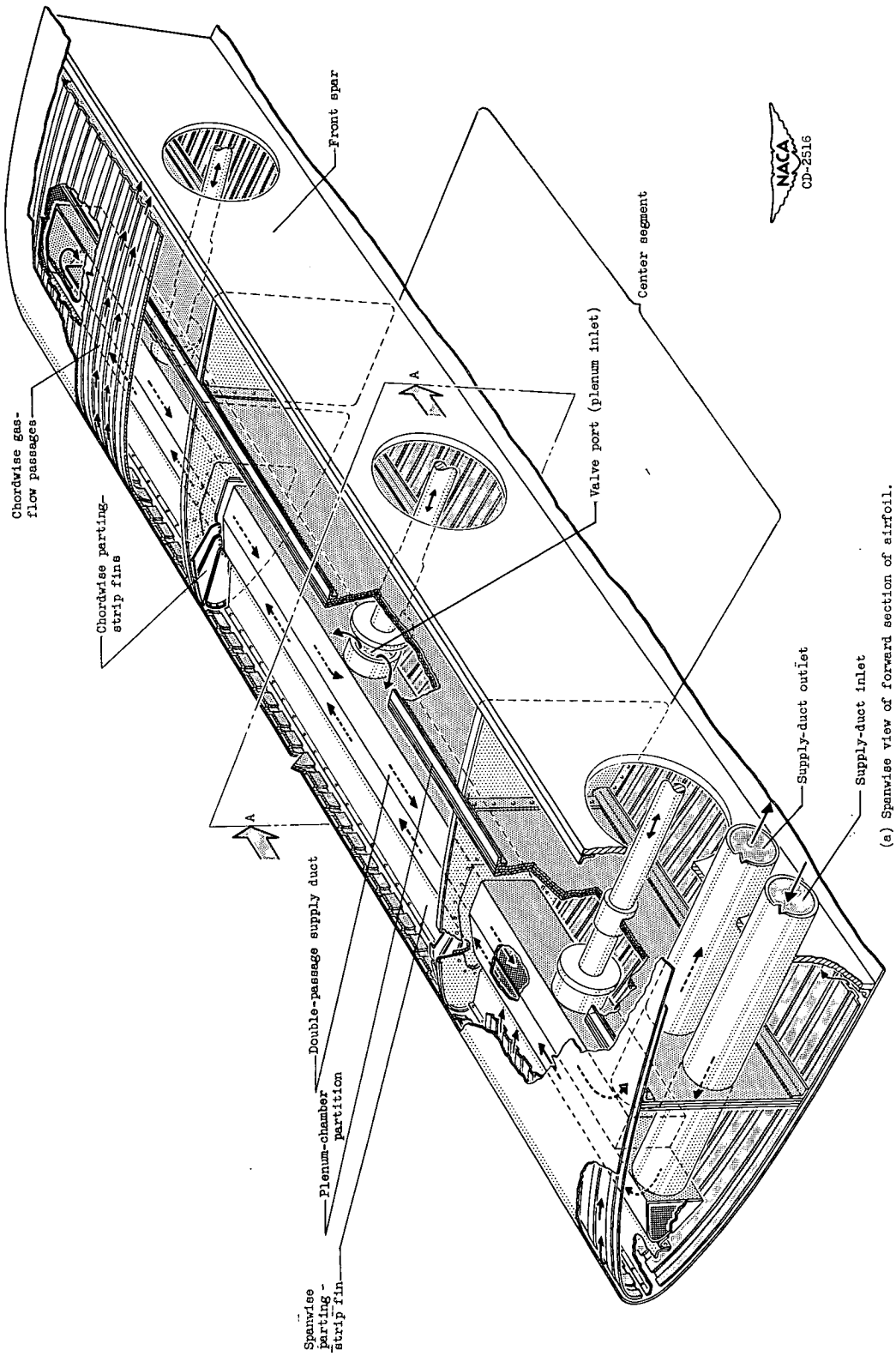

(a) Spanwise view of forward section of airfoil.

Figure 2. - Construction details of gas-heated airfoil for cyclic de-icing.

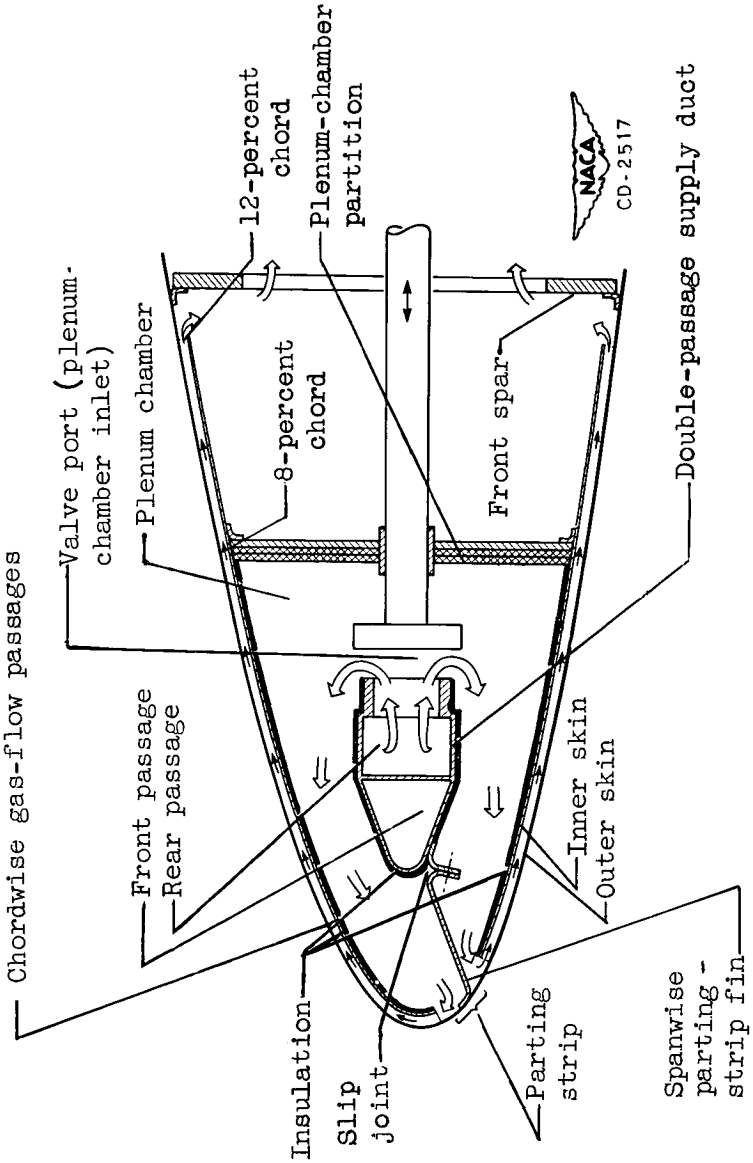

(b) Chordwise cross section A-A.

Figure 2. - Concluded. Construction details of gas-heated airfoil for cyclic de-icing.

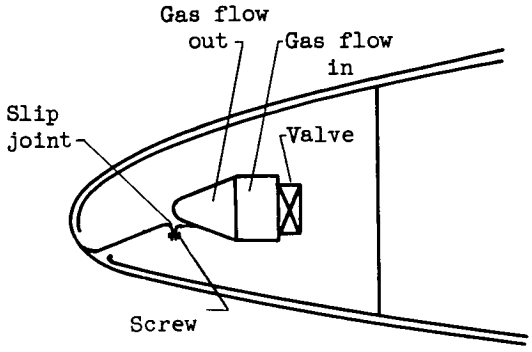

(a) Heating system A. Return-flow gas supply; spanwise and chordwise parting strips.

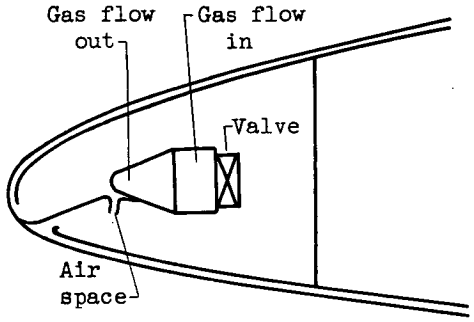

(b) Heating system B. Return-flow gas supply no parting strips.

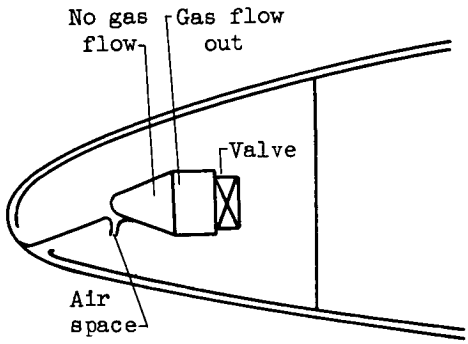

(c) Heating system C. Nonreturn gas supply; no parting strips.

Figure 3. - Schematic diagrams of gas-heating systems for three methods of cyclic de-icing.

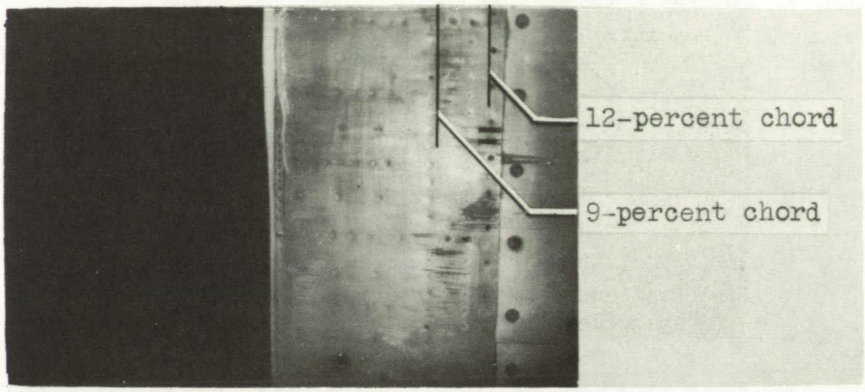

Before heat-on period

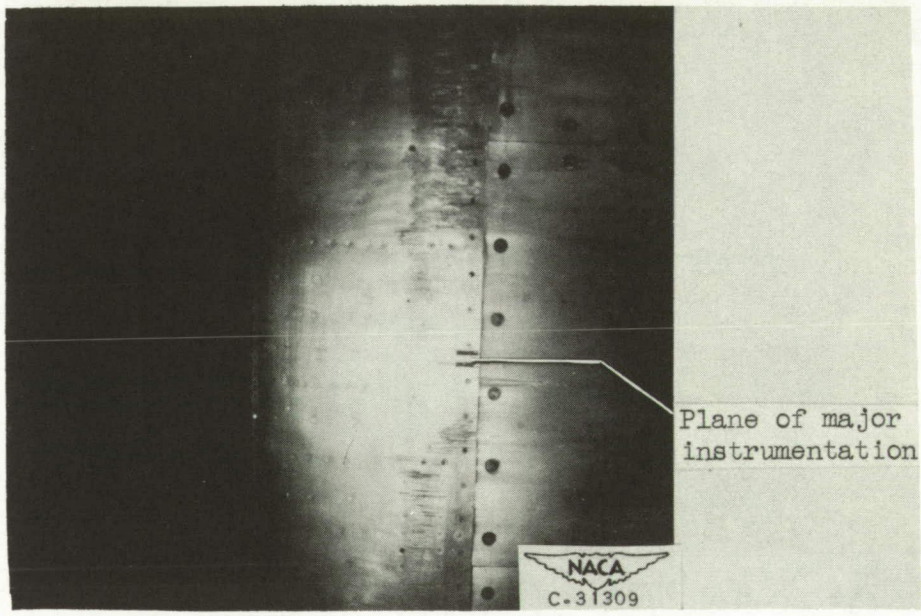

After 20-second heat-on period

(a) Airspeed, 280 miles per hour; datum air temperature, -11° F; liquid-water content, 0.4 gram per cubic meter; angle of attack, 2°; gas flow, 265 pounds per hour per foot span; model-inlet gas temperature, 500° F; heat-off period, 4 minutes; total icing time, 50 minutes; heating system A; lower surface.

Figure 4. - Characteristic ice deposits with marginal operation of de-icing system.

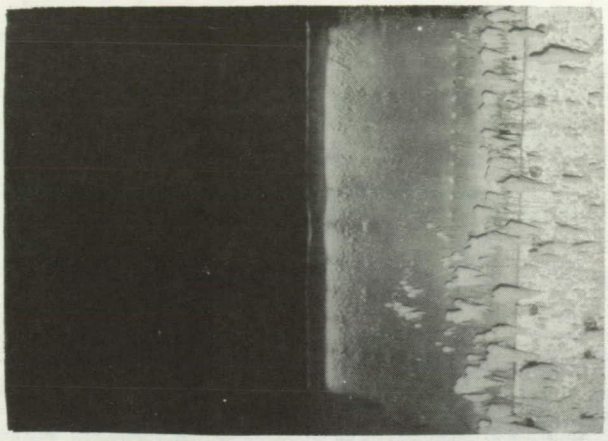

Before heat-on period

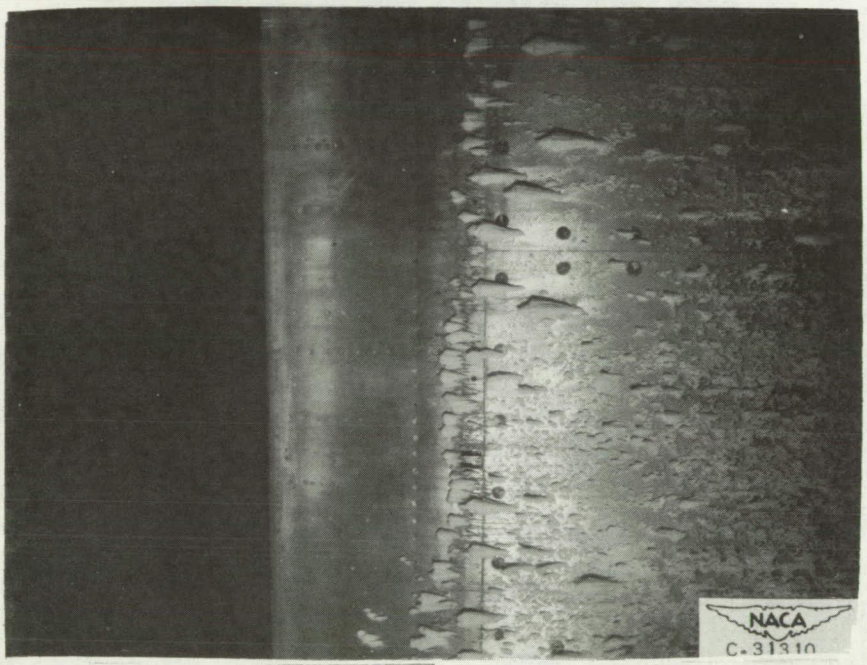

After 15-second heat-on period

(b) Airspeed, 180 miles per hour; datum air temperature, 0° F; liquid-water content, 0.8 gram per cubic meter; angle of attack, 8°; gas flow, 265 pounds per hour per foot span; model-inlet gas temperature, 500° F; heat-off period, 4 minutes; total icing time, 1 hour and 18 minutes; heating system A; lower surface.

Figure 4. - Continued. Characteristic ice deposits with marginal operation of de-icing system.

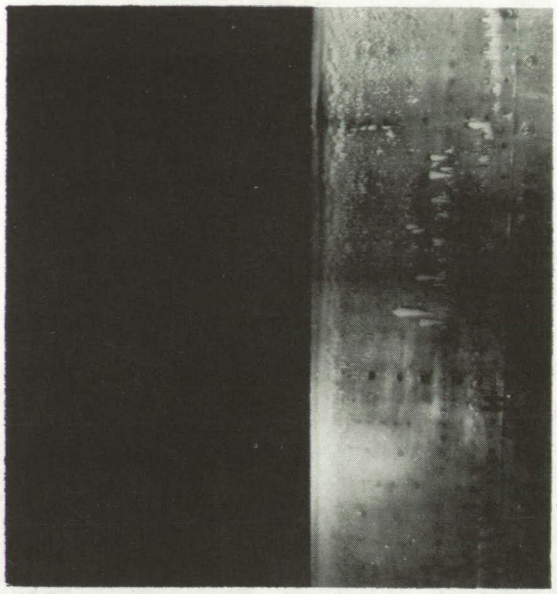

Before heat-on period, lower surface.

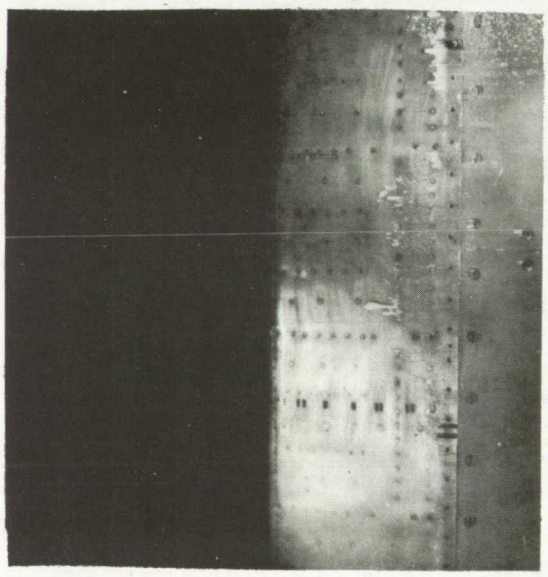

After 10-second heat-on period, lower surface.

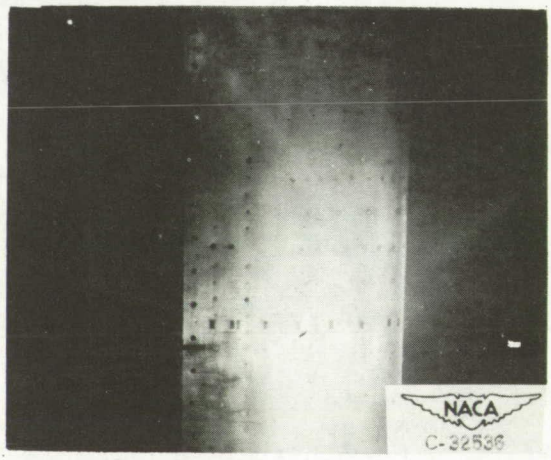

After 10-second heat-on period, upper surface.

(c) Airspeed, 280 miles per hour; datum air temperature, 0° F; liquid-water content, 0.6 gram per cubic meter; angle of attack, 5°; gas flow, 345 pounds per hour per foot span; model-inlet gas temperature, 500° F; heat-off period, 6 minutes; total icing time, 30 minutes; heating system B.

Figure 4. - Continued. Characteristic ice deposits with marginal operation of de-icing system.

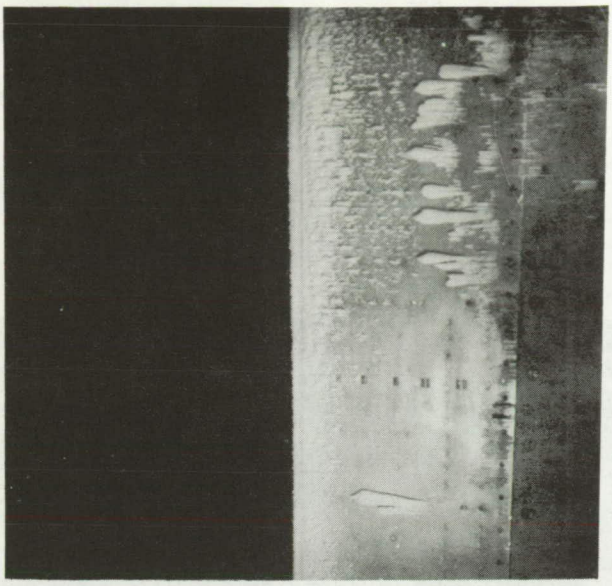

Before heat-on period

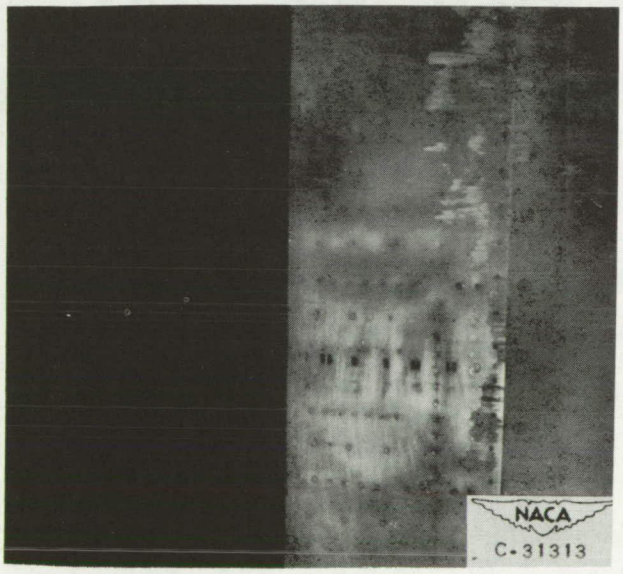

After 35-second heat-on period

(d) Airspeed, 280 miles per hour; datum air temperature, 0° F; liquid-water content, 0.6 gram per cubic meter; angle of attack, 5°; gas flow, 265 pounds per hour per foot span; model-inlet gas temperature, 500° F; heat-off period, 8 minutes; total icing time, 1 hour and 54 minutes; heating system C; lower surface.

Figure 4. - Continued. Characteristic ice deposits with marginal operation of de-icing system.

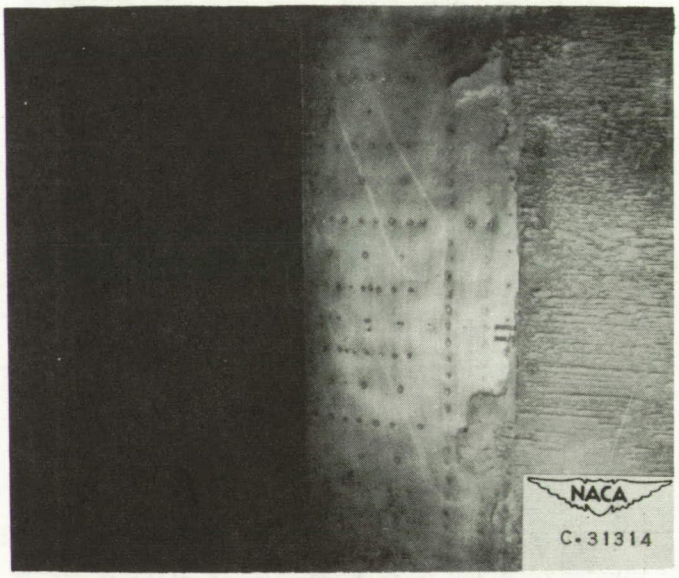

After 45-second heat-on period

(e) Airspeed, 280 miles per hour; datum air temperature, 20° F; liquid-water content, 0.8 gram per cubic meter; angle of attack, 8°; gas flow, 220 pounds per hour per foot span; model-inlet gas temperature, 350° F; heat-off period, 4 minutes; total icing time, 3 hours and 50 minutes; heating system C; lower surface.

Figure 4. - Concluded. Characteristic ice deposits with marginal operation of de-icing system.

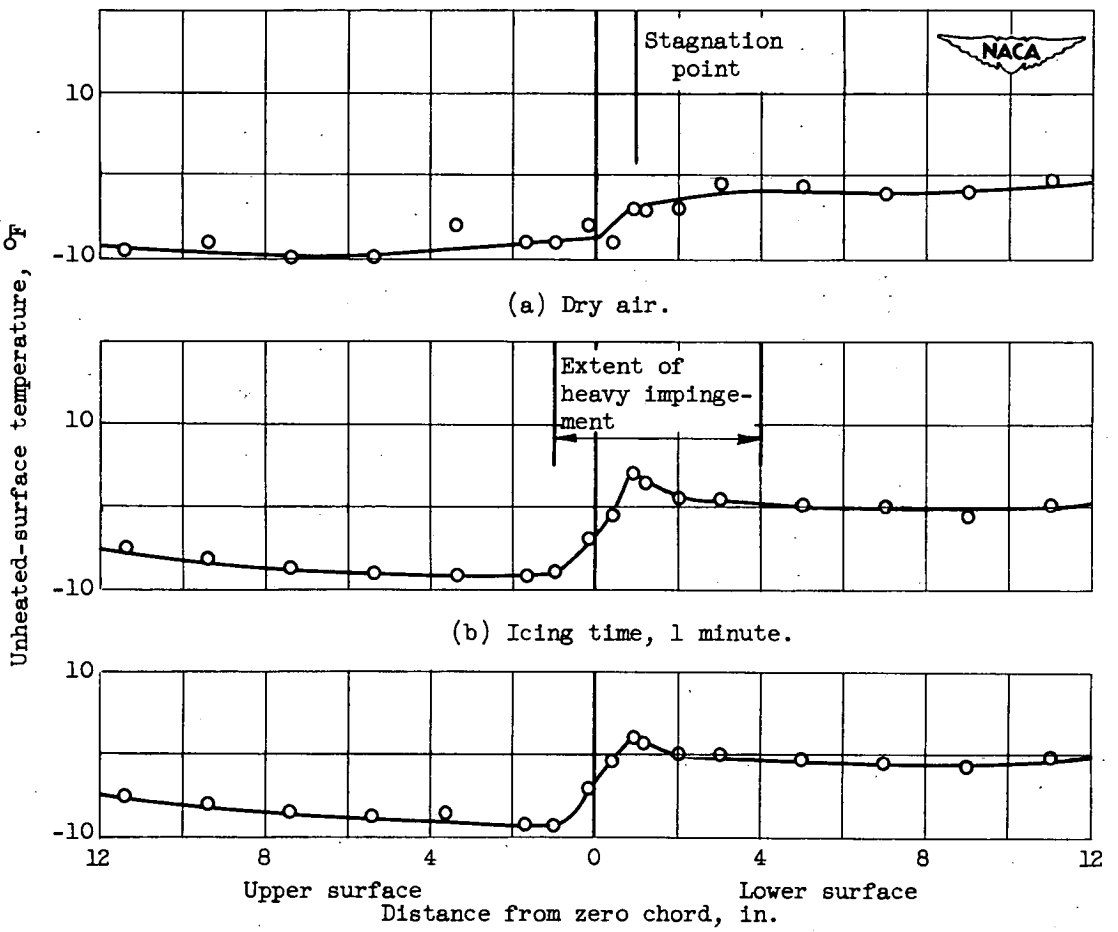

Figure 5. - Chordwise variation of unheated surface temperature in dry air and after start of icing. Airspeed, 280 miles per hour; total air temperature, -2° F; liquid-water content in spray cloud, 0.6 gram per cubic meter; angle of attack, 5°.

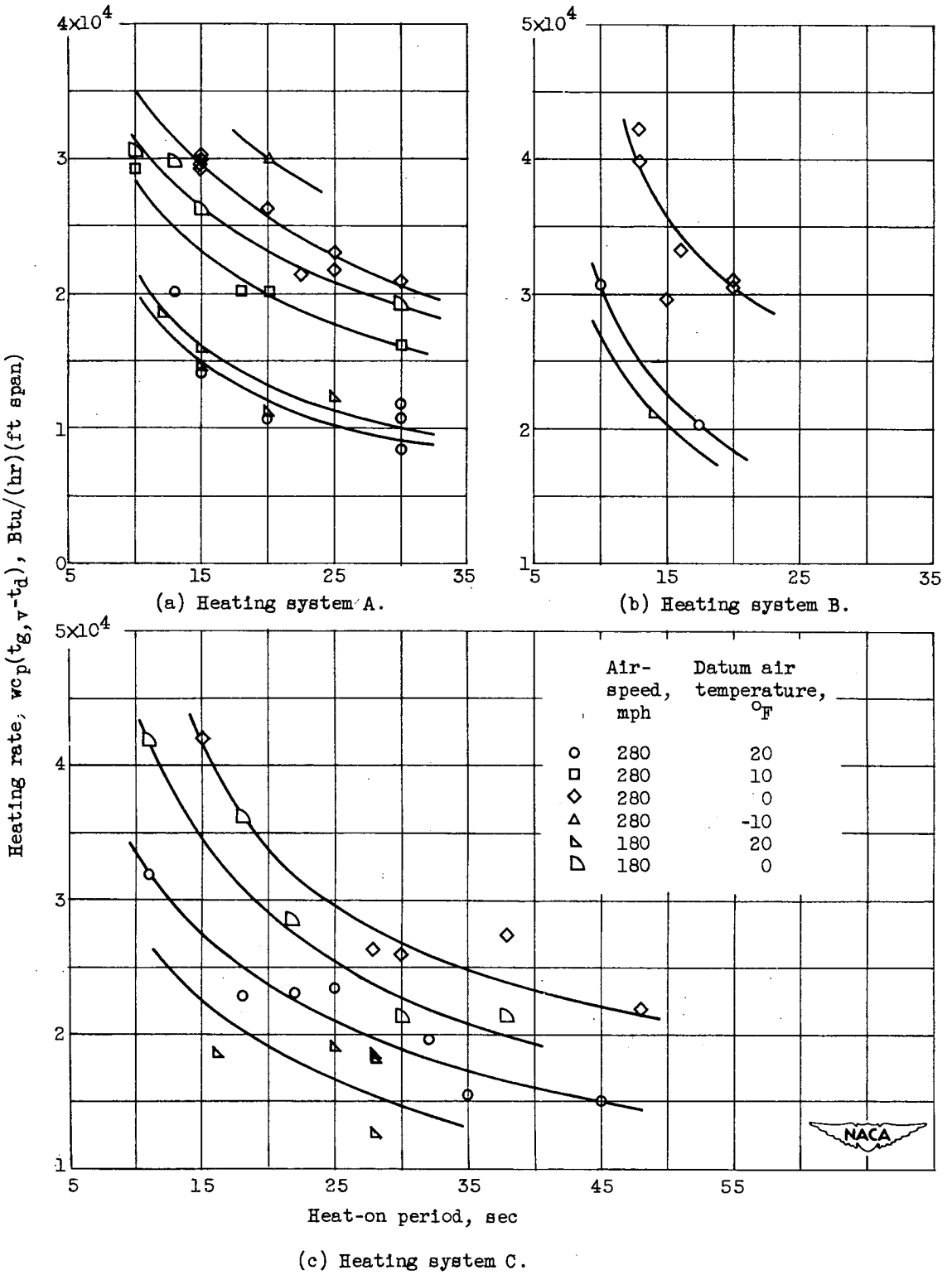

Figure 6. - Variation of heating rate with heat-on period for marginal de-icing. Heat-off period, 4 minutes; nominal liquid-water content.

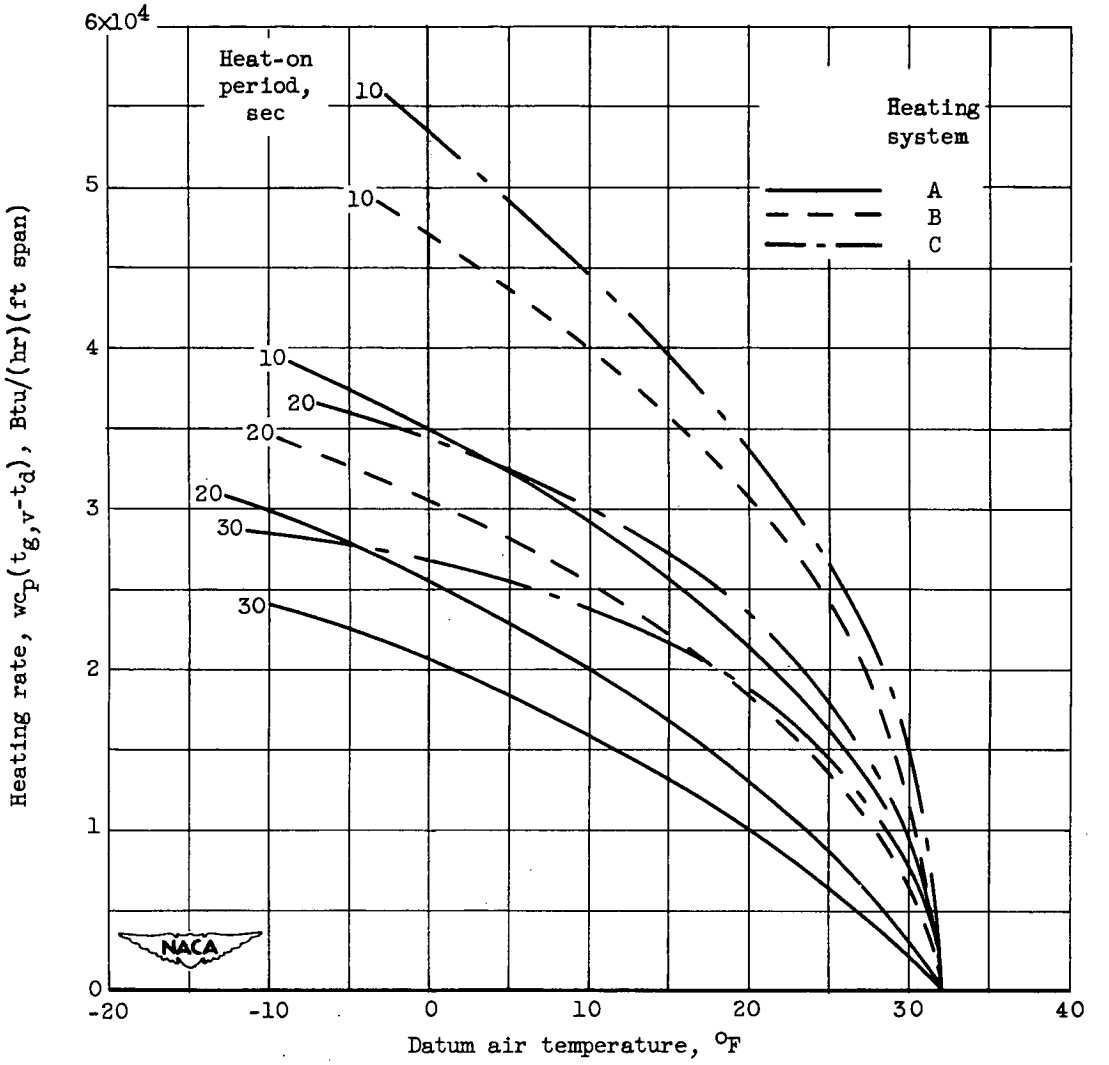

Figure 7. - Variation of heating rate with datum air temperature. Airspeed, 280 miles per hour; heat-off period, 4 minutes; nominal liquid-water content.

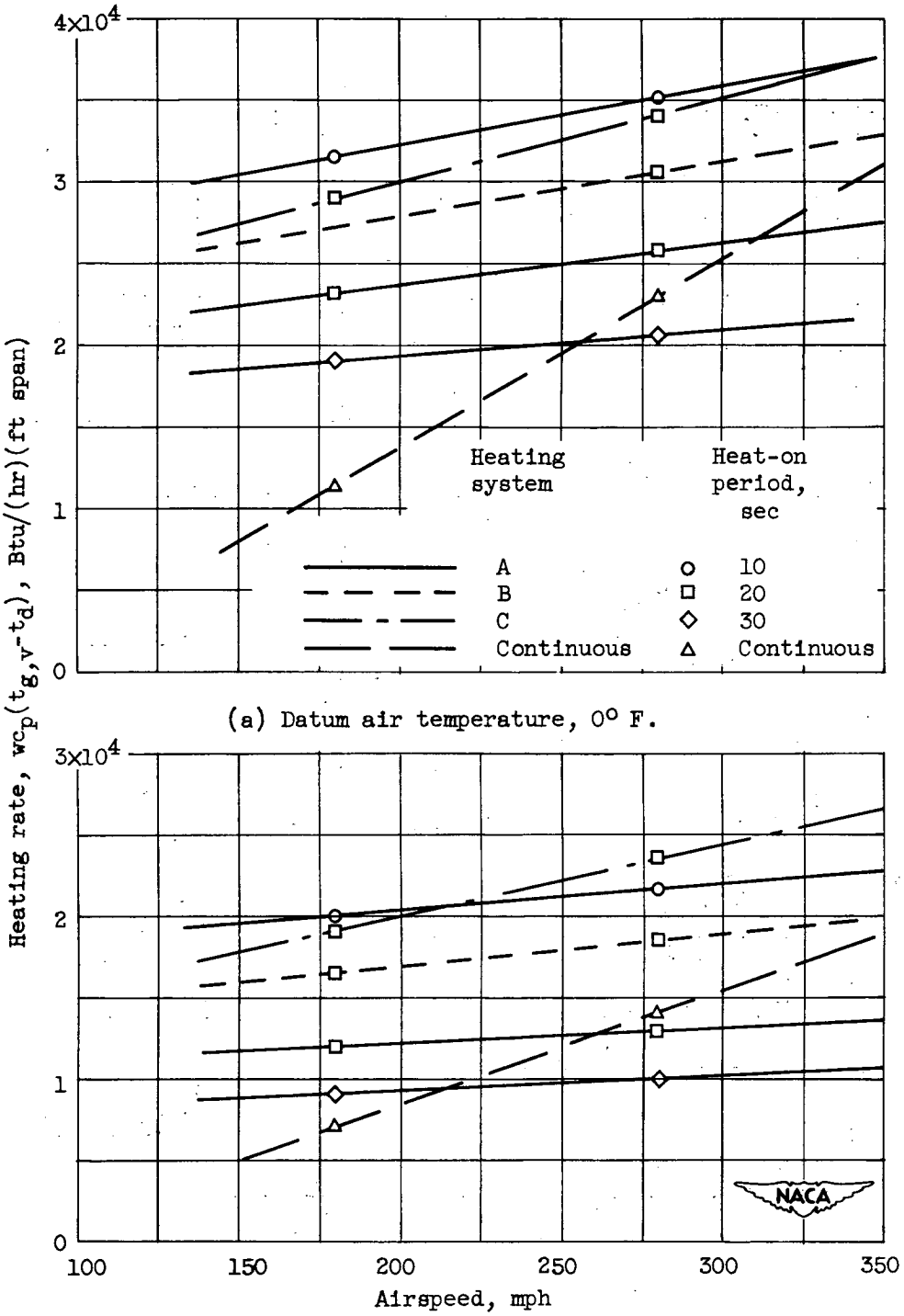

Figure 8. - Variation of heating rate with airspeed for cyclic de-icing and continuous anti-icing. Heat-off period, 4 minutes; nominal liquid-water content.

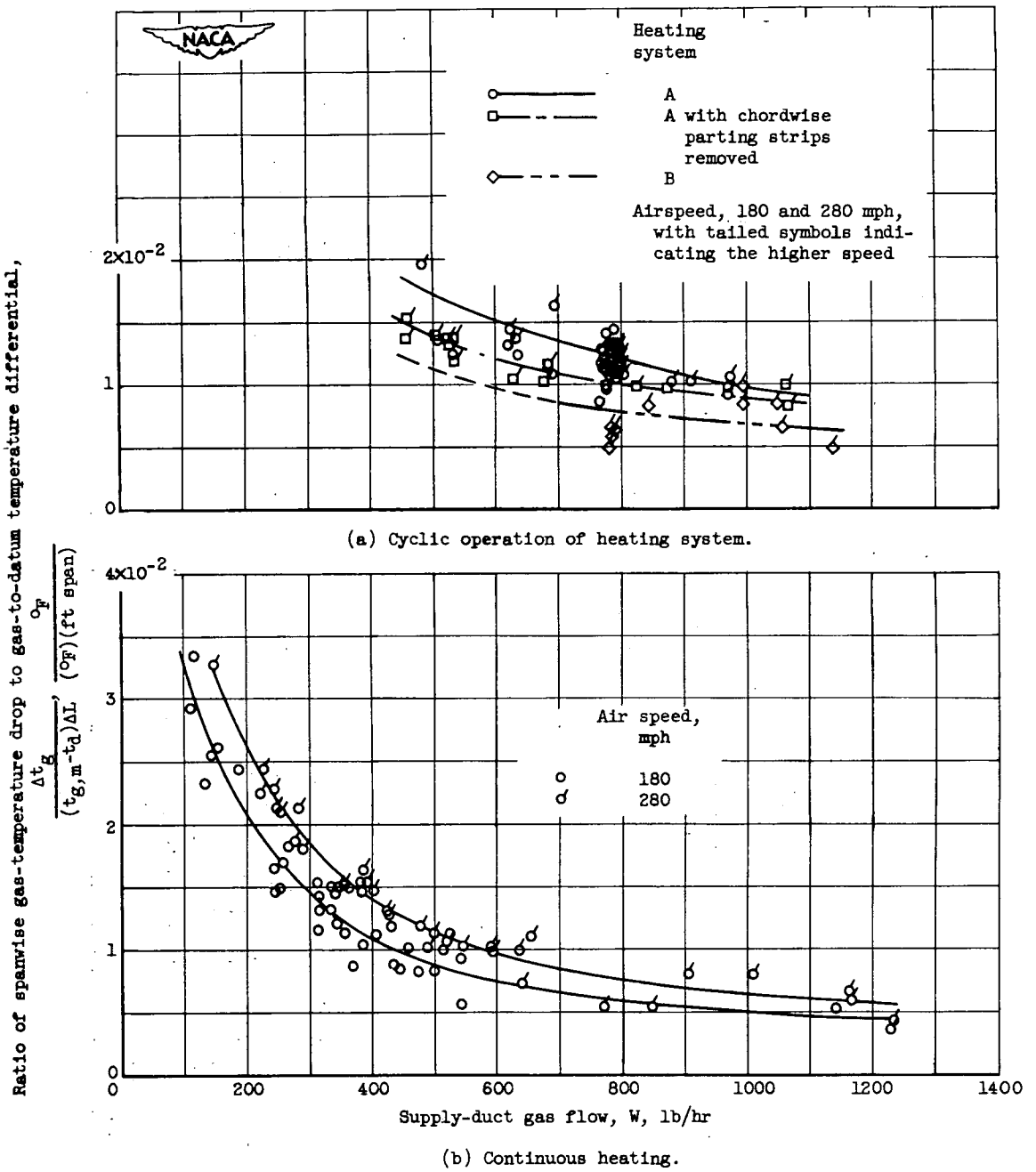

Figure 9. - Spanwise gas-temperature drop as function of gas flow and gas-to-datum temperature differential.

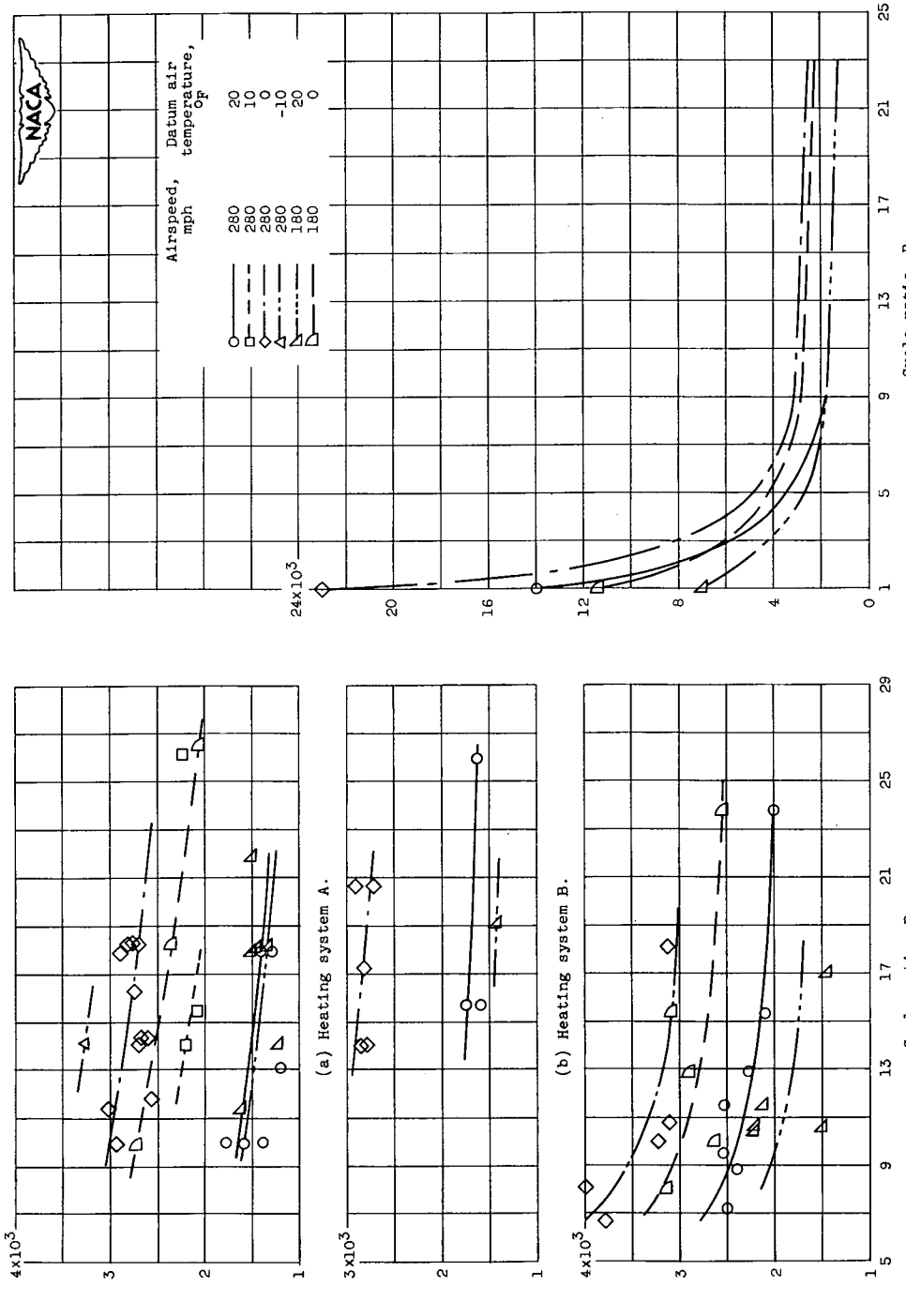

Figure 10. - Equivalent-continuous heating requirement per foot span as function of cycle ratio. Heat-off period, approximately $4\frac{1}{3}$ minutes; nominal liquid-water content.

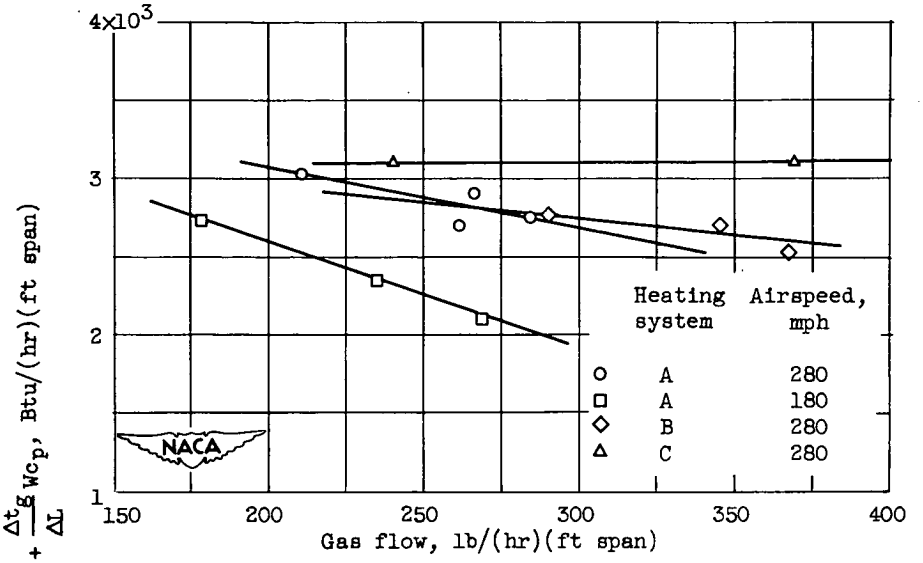

(a) Effect of gas flow. Gas temperature at valve, approximately 460° F; angle of attack, 5°; icing period, 4 minutes.

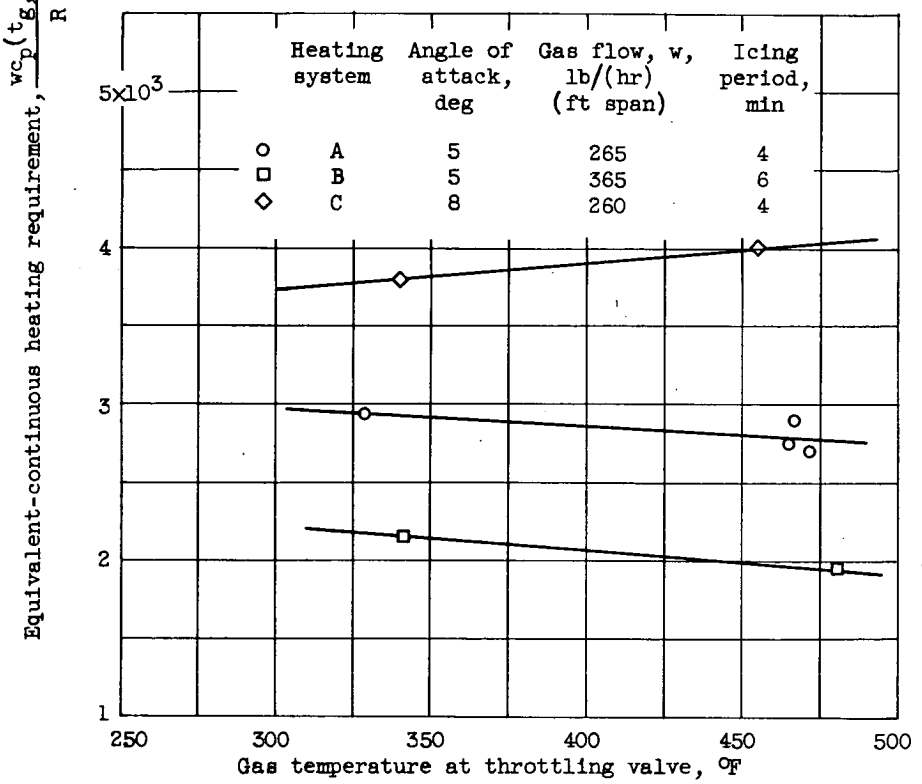

(b) Effect of gas temperature. Airspeed, 280 miles per hour.

Figure 11. - Effect of gas flow and temperature on equivalent-continuous heating requirement. Datum air temperature, 0° F; liquid-water content, 0.6 gram per cubic meter.

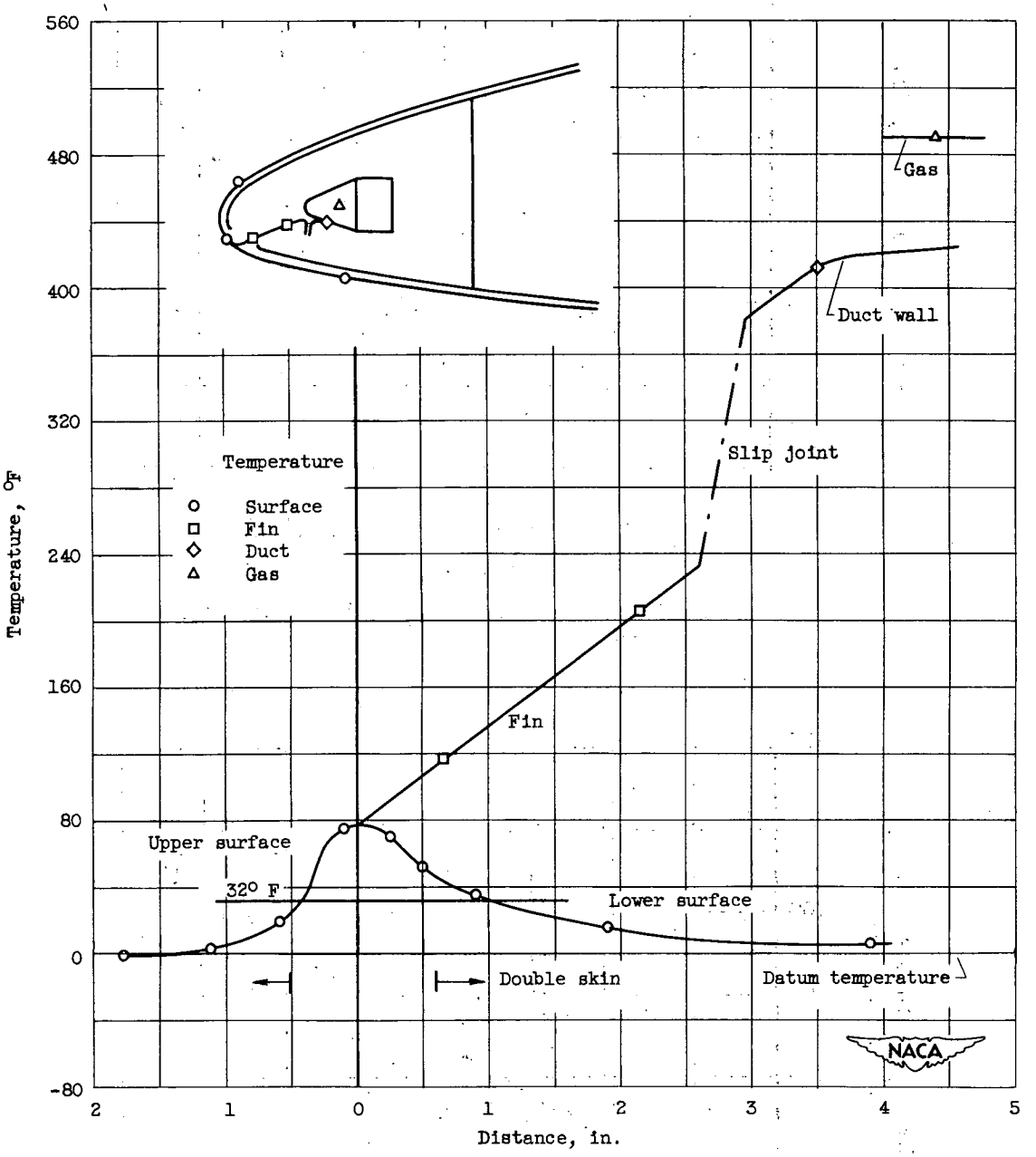

Figure 12. - Typical temperature pattern pertaining to spanwise parting strip and adjacent airfoil surface. Airspeed, 280 miles per hour; datum air temperature, 0° F; liquid-water content, 0.6 gram per cubic meter; angle of attack, 5°; supply-duct gas flow, 800 pounds per hour; icing period, 4 minutes; heating system A.

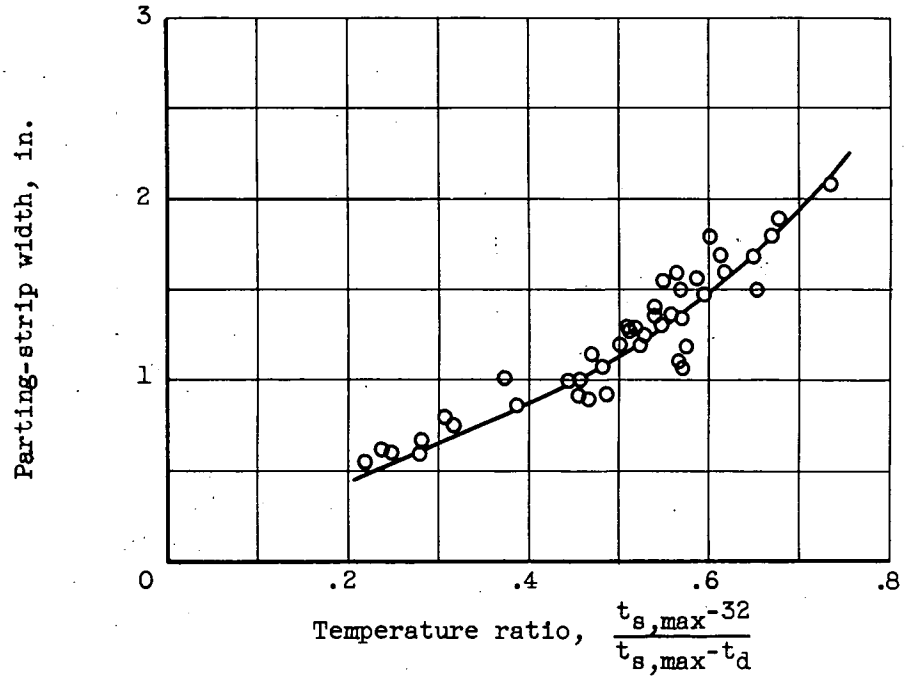

Figure 13. - Parting-strip width as function of temperature ratio.

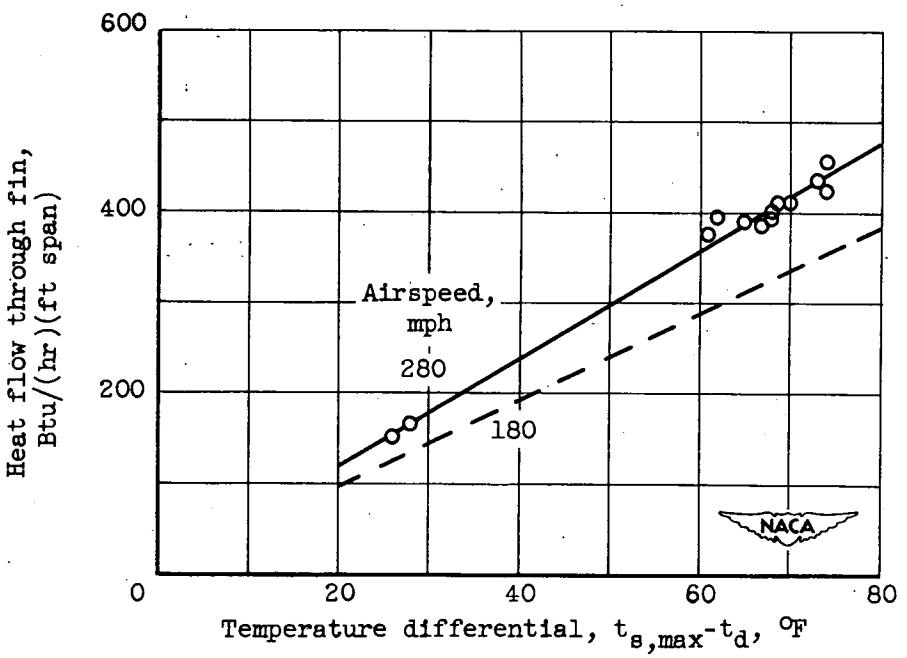

Figure 14. - Correlation of maximum parting-strip temperature with heat flow through fin.

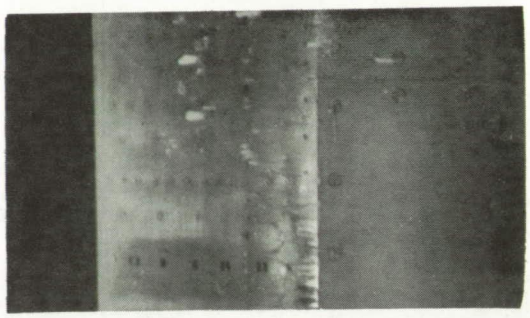

(a) Runback icing after ice removal of third (short) cycle. Heat-on period, 13 seconds; heat-off period, $4\frac{1}{3}$ minutes; total time in icing, 2 hours and 42 minutes.

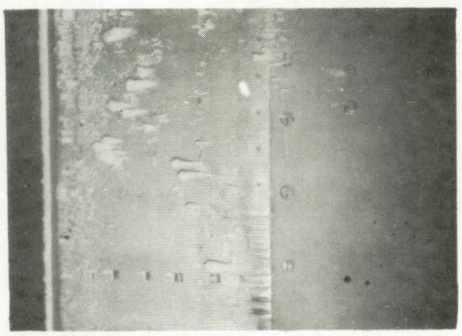

(b) Primary and runback icing before ice removal of fourth (long) cycle. Heat-off period, 7 minutes.

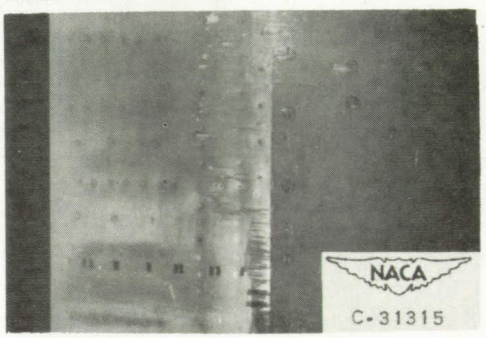

(c) Runback icing after 21-second heat-on period (fourth cycle). Total icing time, 2 hours and 49 minutes.

Figure 15. - Reduction of runback icing by secondary cycling. Airspeed, 280 miles per hour; datum air temperature, 0° F; liquid-water content, 0.6 gram per cubic meter; angle of attack, 5°; gas flow, 265 pounds per hour per foot span; model-inlet gas temperature, 500° F; lower surface.

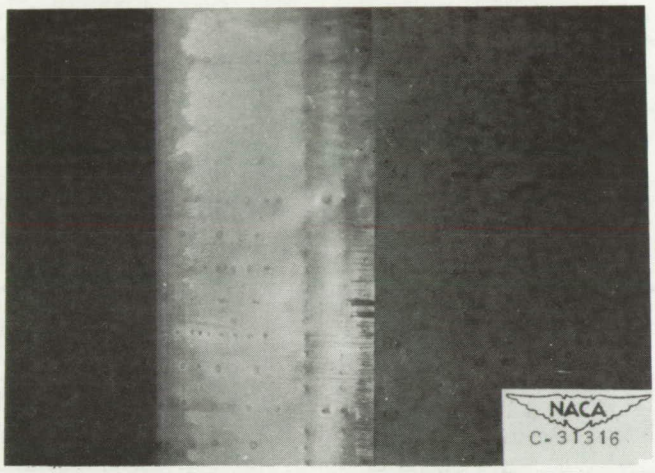

Figure 16. - Residual ice on lower airfoil surface following a marginal heating cycle to a cold and iced airfoil with 1 minute of supply-duct preheating time. Airspeed, 280 miles per hour; datum air temperature, 0° F; liquid-water content, 0.6 gram per cubic meter; angle of attack, 5°; supply-duct gas flow, 800 pounds per hour; gas temperature 5 feet upstream of model inlet, 500° F; heat-on period, 15 seconds; total icing time, 5 minutes; heating system A.

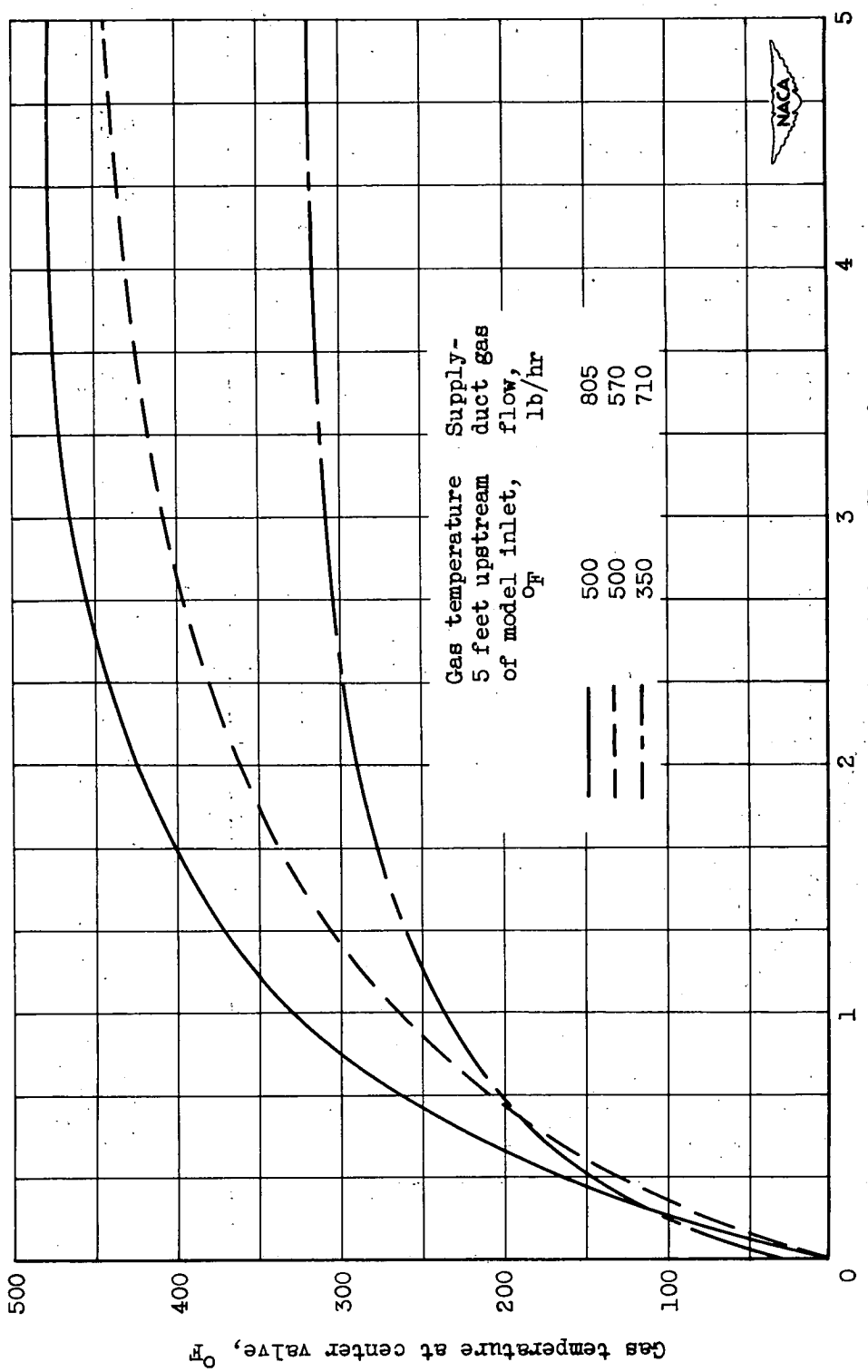

Figure 17. - Variation of gas temperature at center valve with time after start of hot-gas flow. Airspeed, 280 miles per hour; datum air temperature, 0° F; liquid-water content, 0.6 gram per cubic meter; angle of attack, 5°; heating system A.

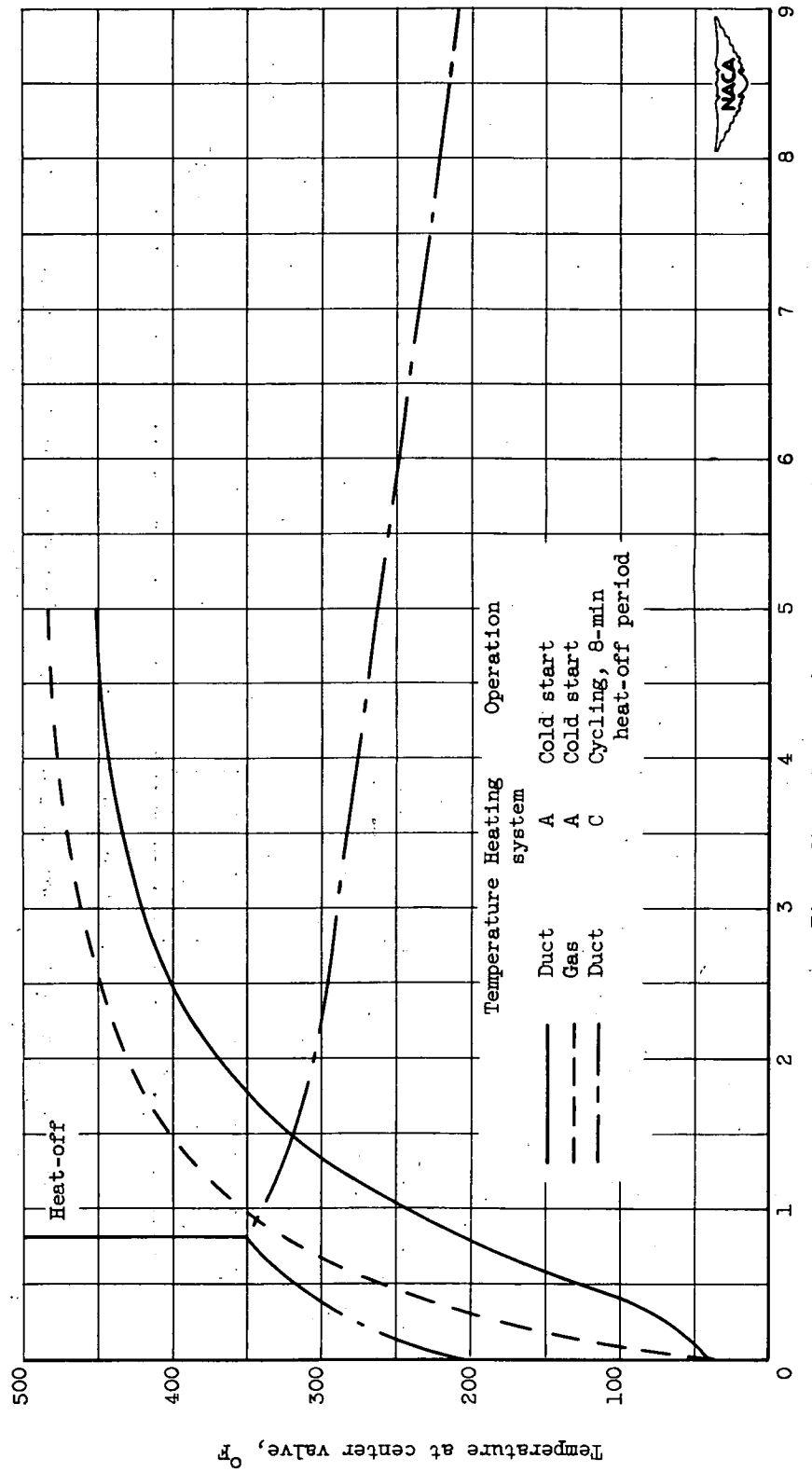

Figure 18. - Comparison of heating and cooling rates for gas and duct temperatures at center valve for heating systems A and C. Airspeed, 280 miles per hour; datum air temperature, 0° F; liquid-water content, 0.6 gram per cubic meter; angle of attack, 5°; gas temperature 5 feet upstream of model inlet, 500° F; supply-duct gas flow, 805 pounds per hour.

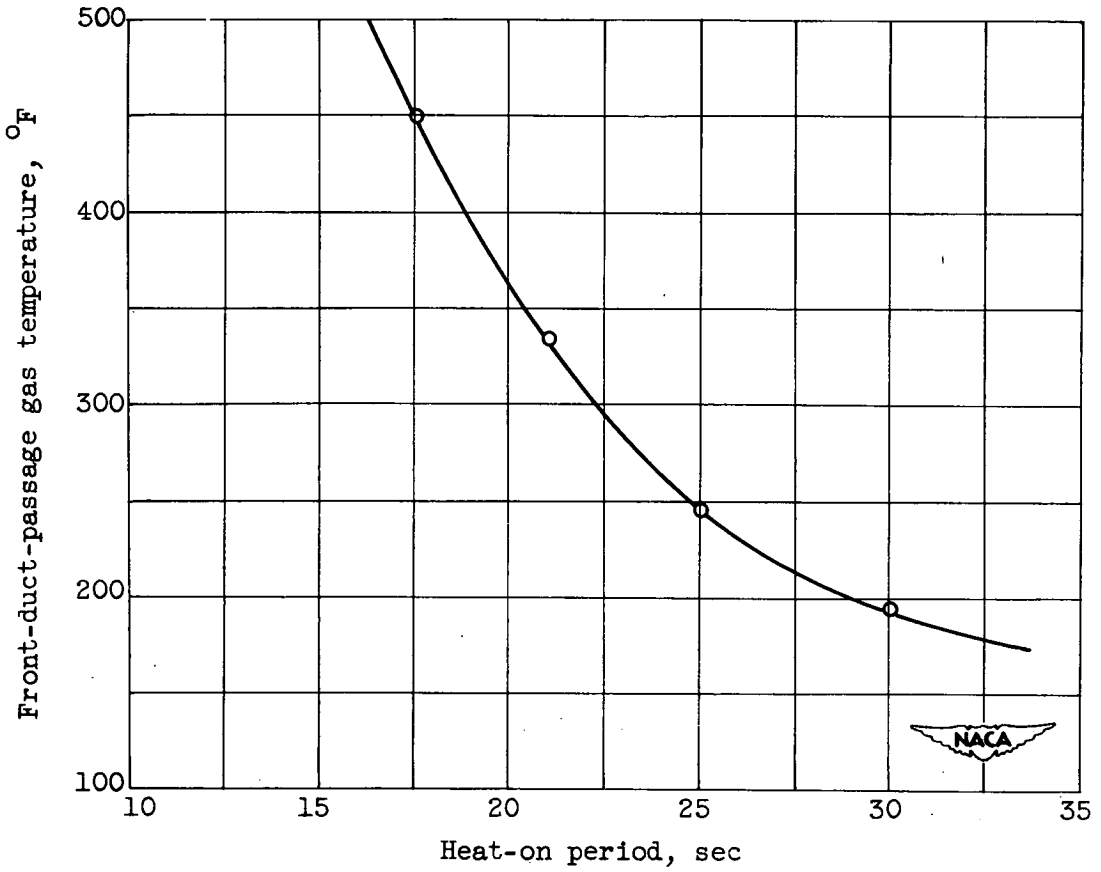

Figure 19. - Heat-on period for marginal de-icing as function of gas temperature in front duct passage. Airspeed, 280 miles per hour; datum air temperature, 0° F; liquid-water content, 0.6 gram per cubic meter; angle of attack, 5°; rear-passage gas flow, 265 pounds per hour per foot span; front-passage gas flow, 500 to 800 pounds per hour; rear-passage inlet-gas temperature, 500° F; icing period, 4 minutes.

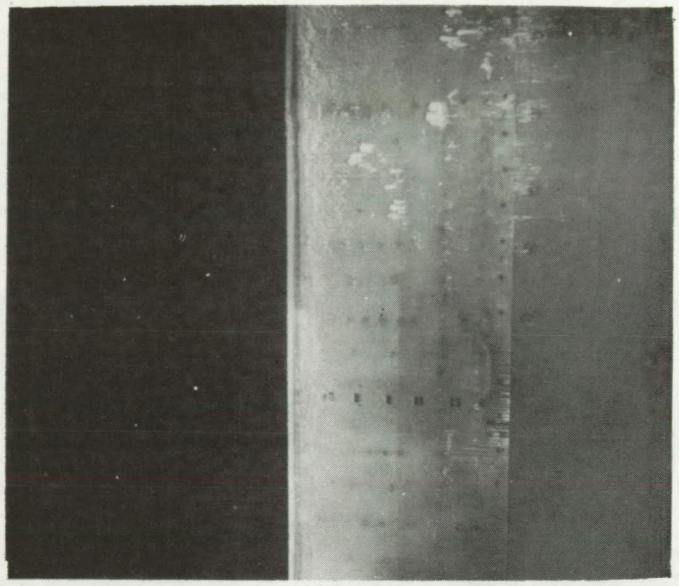

(a) After 4-minute icing period.

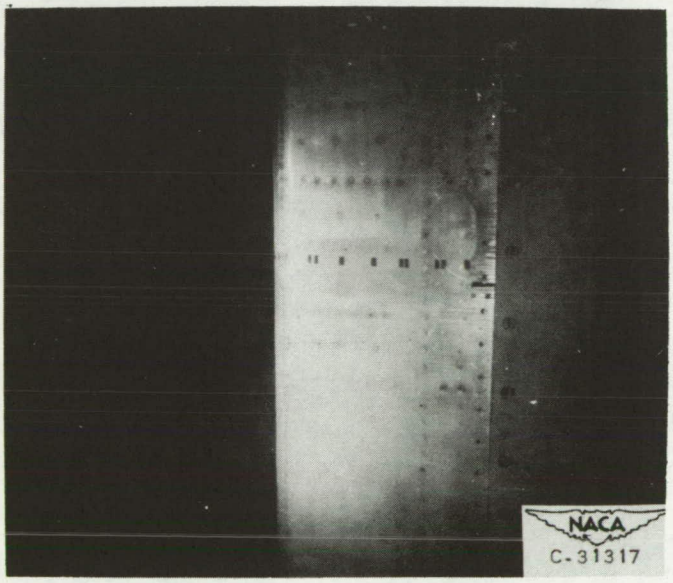

(b) After 30-second heat-on period.

Figure 20. - Cyclic de-icing with spanwise parting-strip fin attached to duct and no flow in front passage. Airspeed, 280 miles per hour; datum air temperature, 0° F; angle of attack, 5°; liquid-water content, 0.6 gram per cubic meter; rear-passage gas flow, 265 pounds per hour per foot span; rear-passage inlet-gas temperature, 500° F; total icing time, 1 hour and 9 minutes; lower surface.

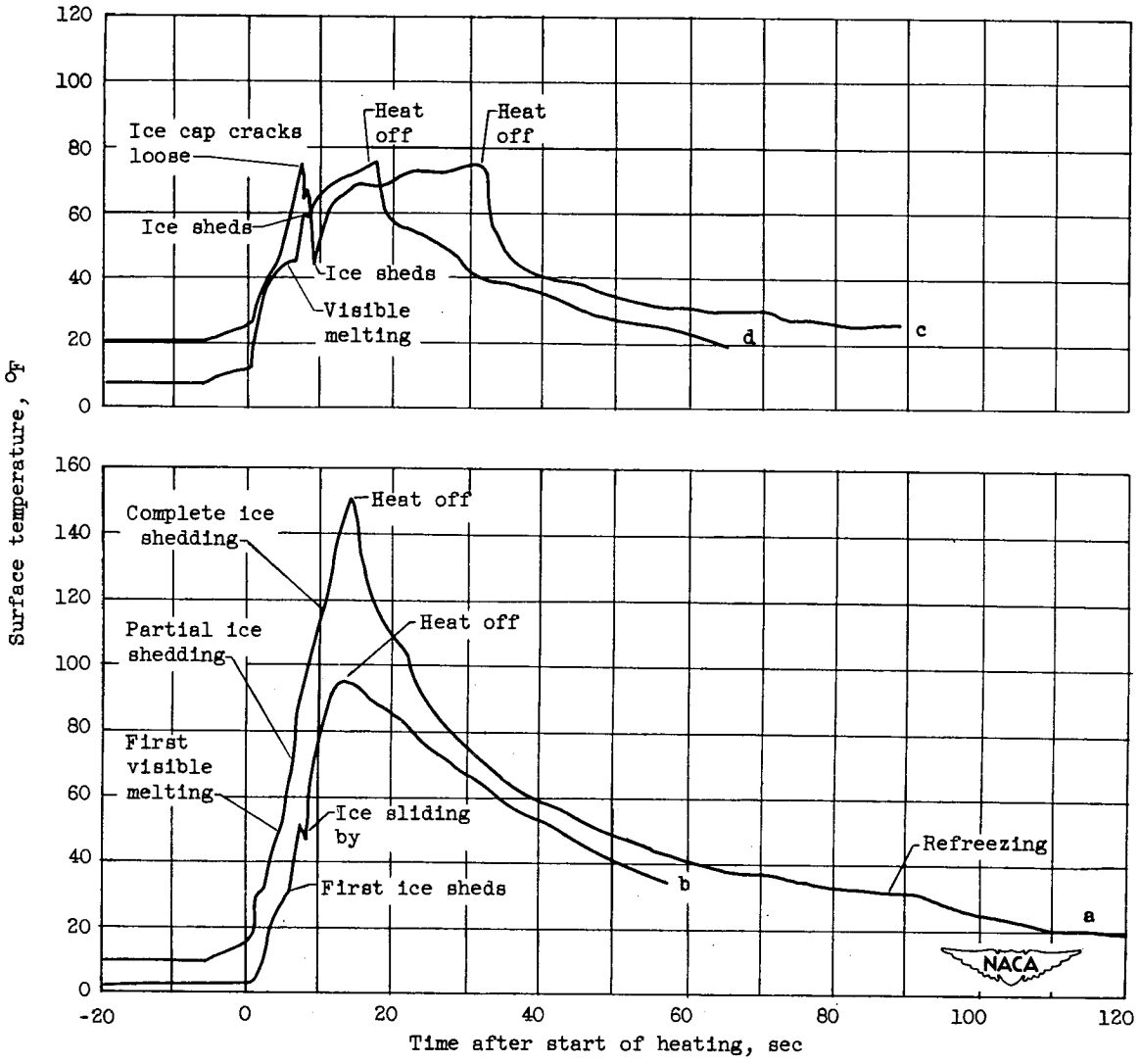

Figure 21. - Several surface temperature-time curves showing melting and shedding of ice. Conditions listed in table II.

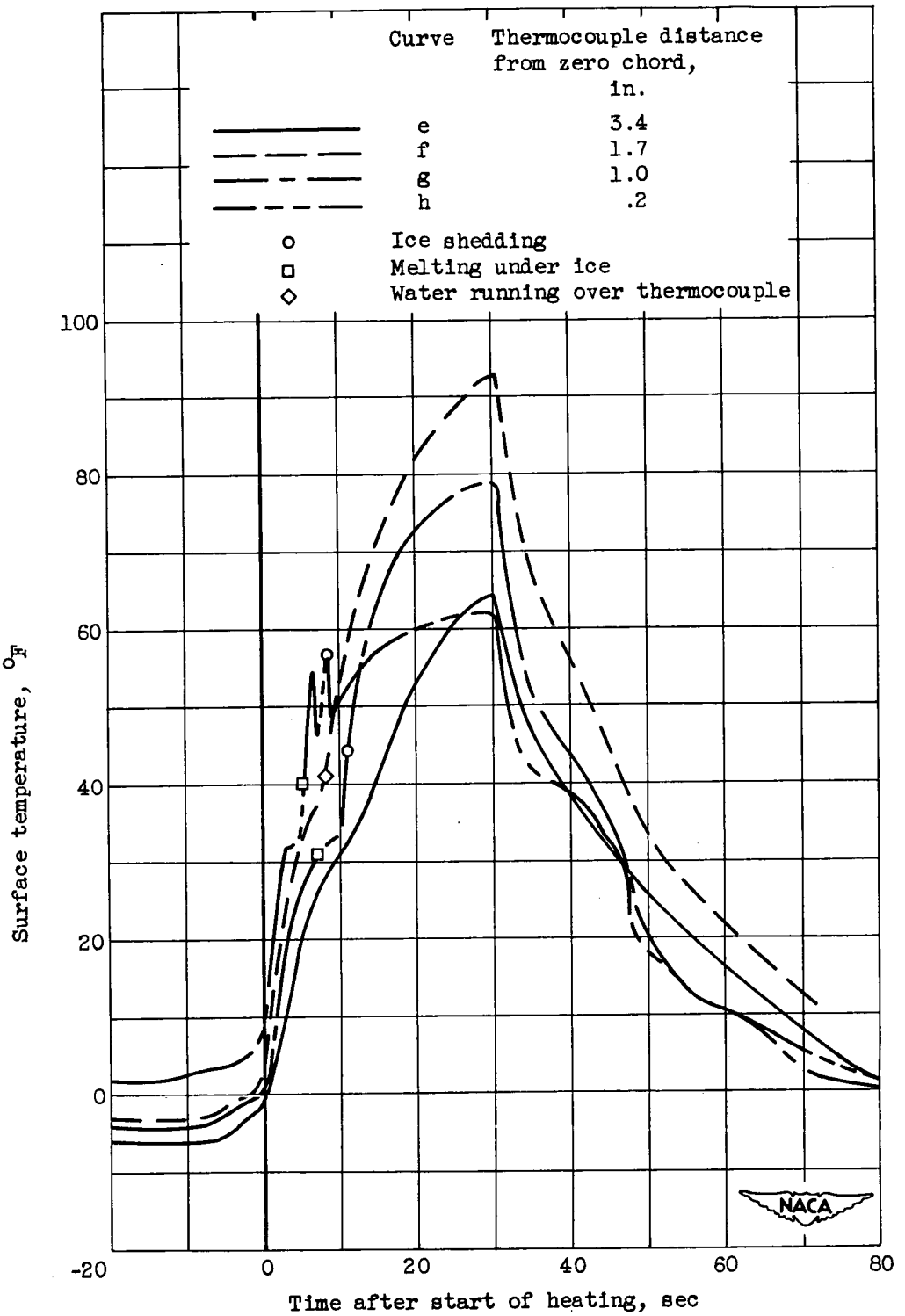

Figure 22. - Simultaneous temperature-time curves for four upper-surface thermocouples. Conditions listed in table II.

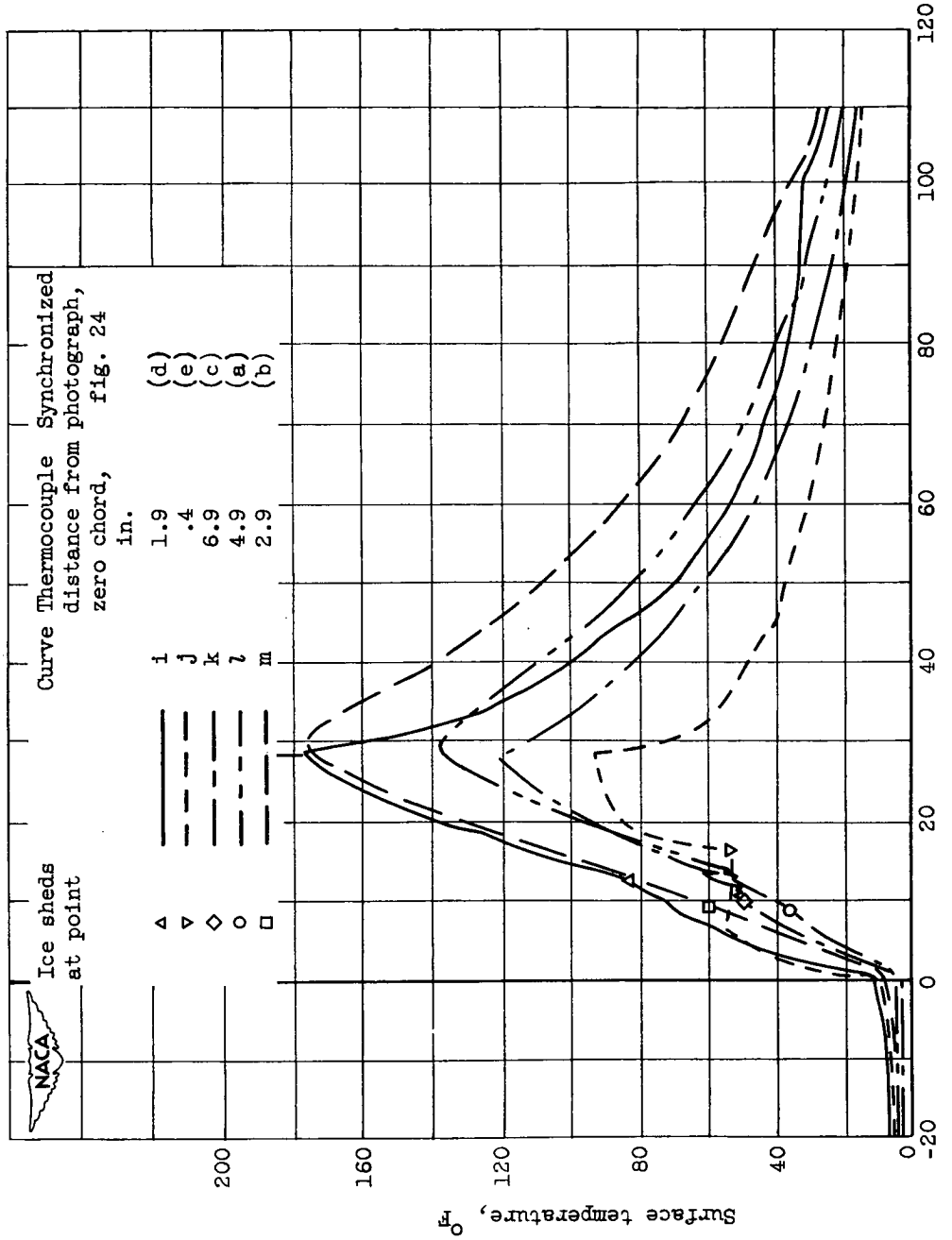

Figure 23. - Time variation of surface temperature over lower surface, showing time of shedding. Conditions listed in table II.

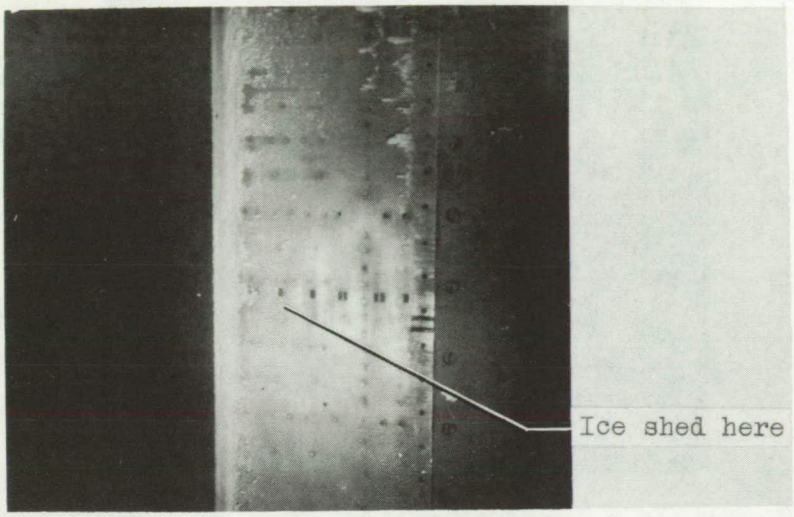

(a) Heating time, 8 seconds.

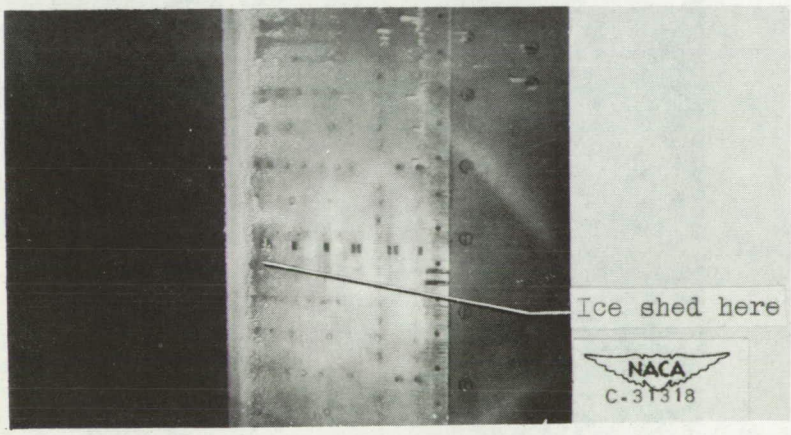

(b) Heating time, 9 seconds.

Figure 24. - Photographs of ice shedding from lower surface synchronized with surface-temperature curves of figure 23. Conditions listed in table II.

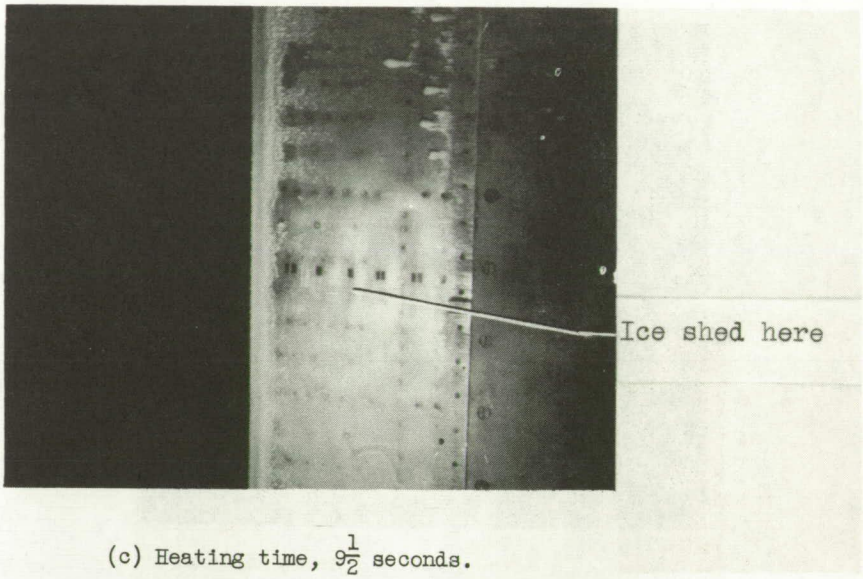

(c) Heating time, $9\frac{1}{2}$ seconds.

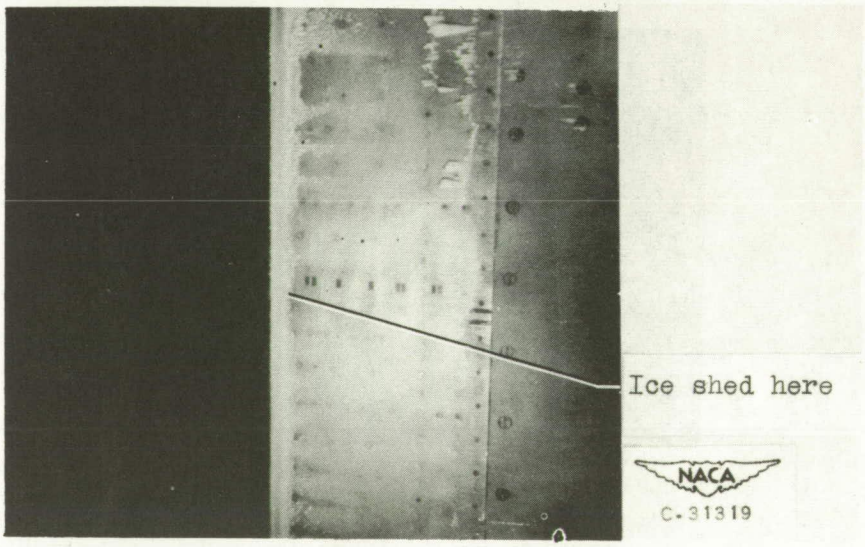

(d) Heating time, 12 seconds.

Figure 24. - Continued. Photographs of ice shedding from lower surface synchronized with surface-temperature curves of figure 23. Conditions listed in table II.

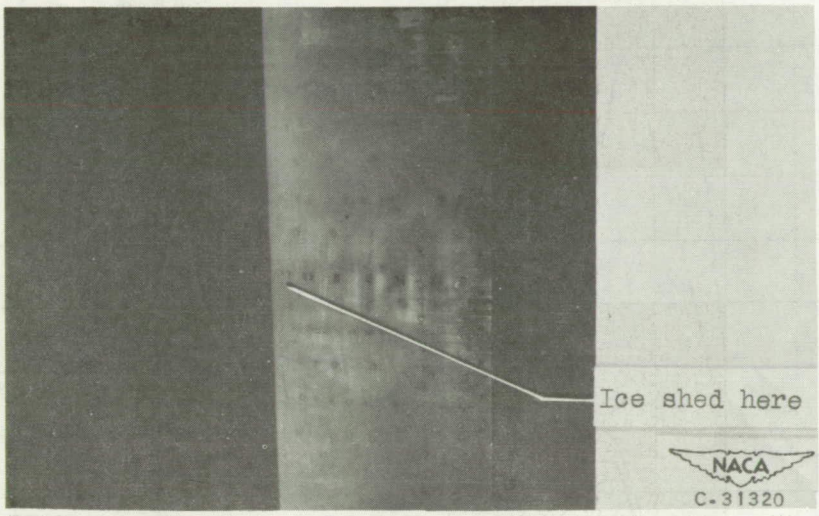

(e) Heating time, $16\frac{1}{2}$ seconds.

Figure 24. - Concluded. Photographs of ice shedding from lower surface synchronized with surface-temperature curves of figure 23. Conditions listed in table II.

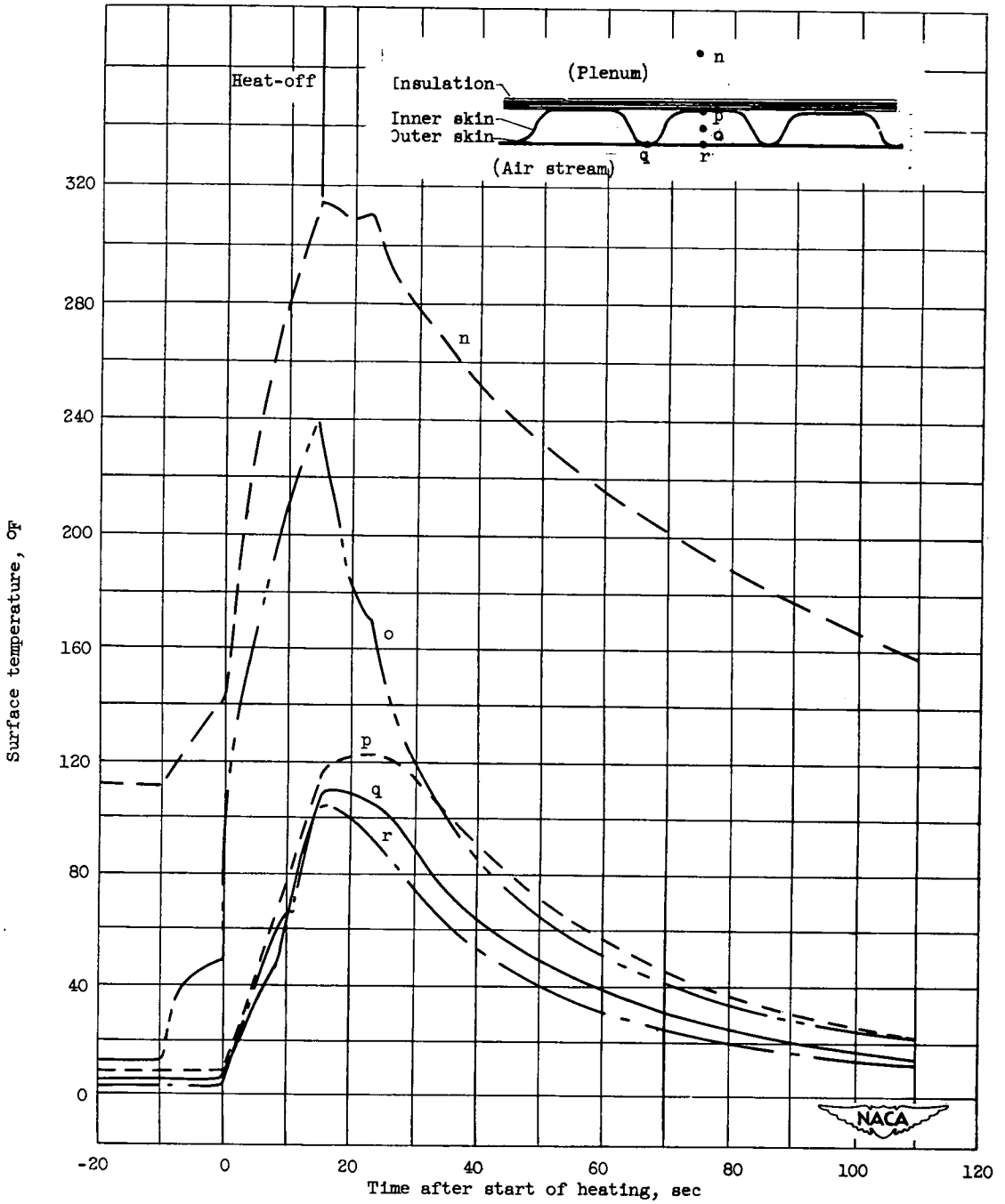

Figure 25. - Temperature variations about a typical double-skin chordwise passage. Conditions listed in table II.

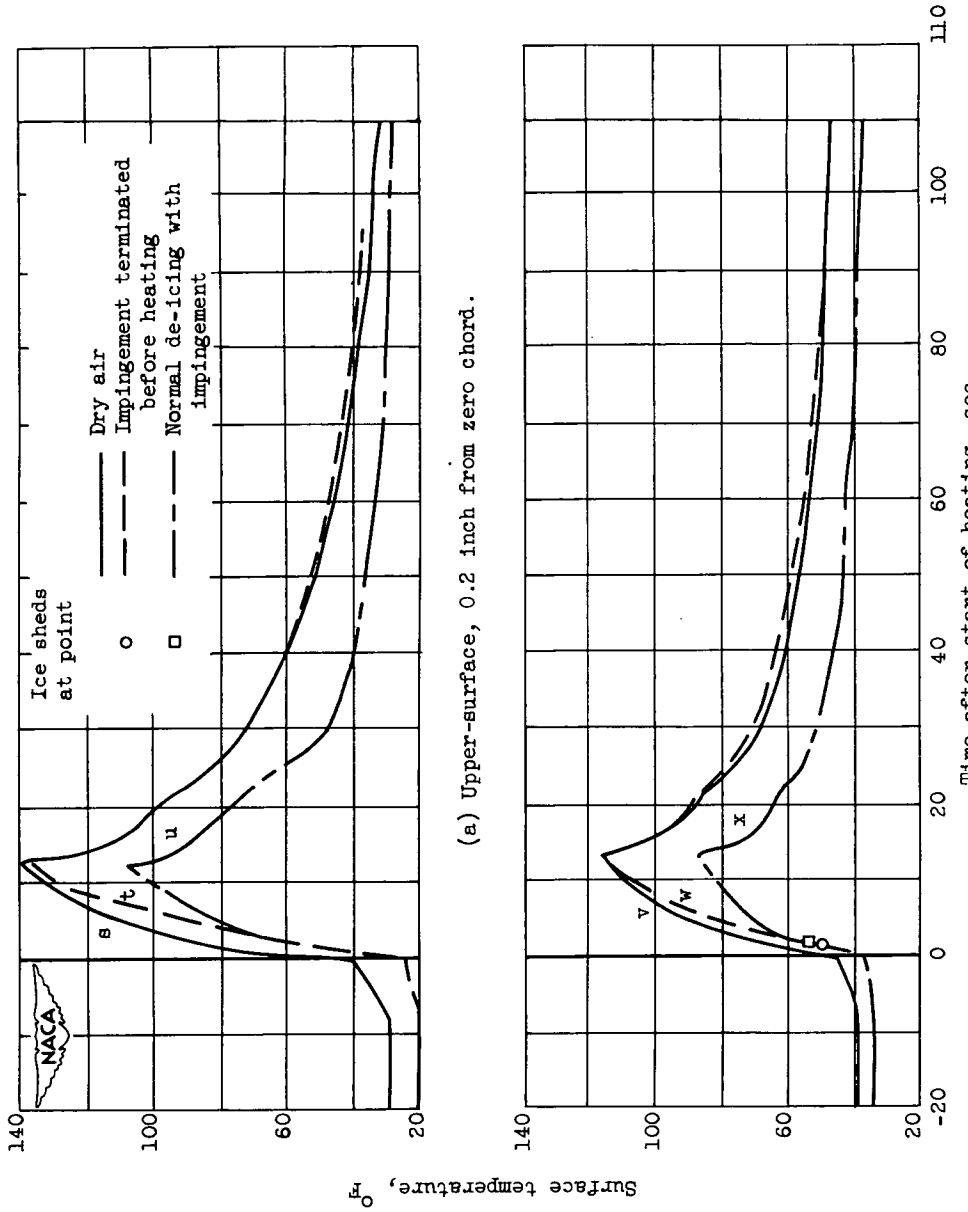

(a) Upper-surface, 0.2 inch from zero chord.

(b) Lower-surface, 0.4 inch from zero chord.

Figure 26. - Comparison of surface-temperature curves in dry air, normal de-icing, and de-icing without impingement. Conditions listed in table II.

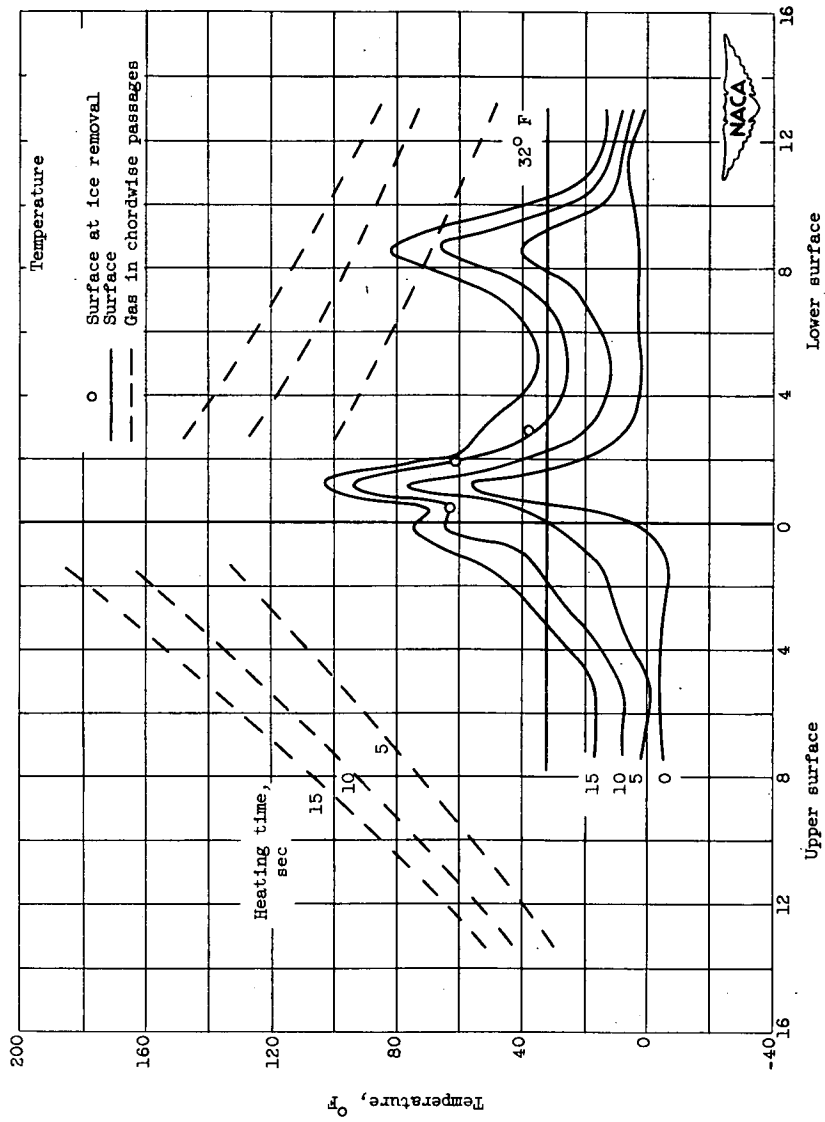

(a) Gas flow, 153 pounds per hour per foot span.

Figure 27. - Chordwise variation of surface and gas temperature during heating period with temperature at time of ice removal. Airspeed, 280 miles per hour; datum air temperature, 0° F; liquid-water content, 0.6 gram per cubic meter; angle of attack, 5°; model-inlet gas temperature, 500° F; heating system A.

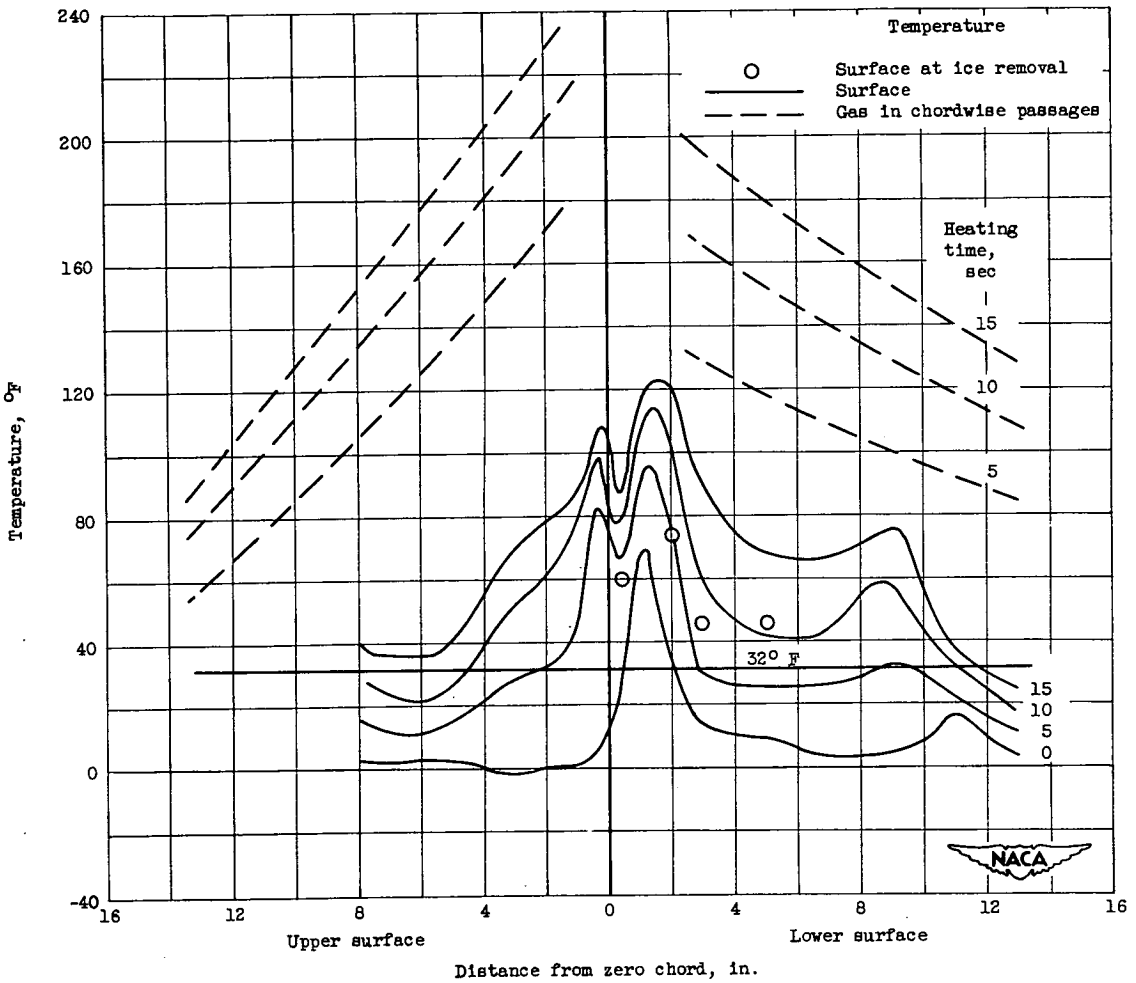

(b) Gas flow, 233 pounds per hour per foot span.

Figure 27. - Continued. Chordwise variation of surface and gas temperature during heating period with temperature at time of ice removal. Airspeed, 280 miles per hour; datum air temperature, 0° F; liquid-water content, 0.6 gram per cubic meter; angle of attack, 5°; model-inlet gas temperature, 500° F; heating system A.

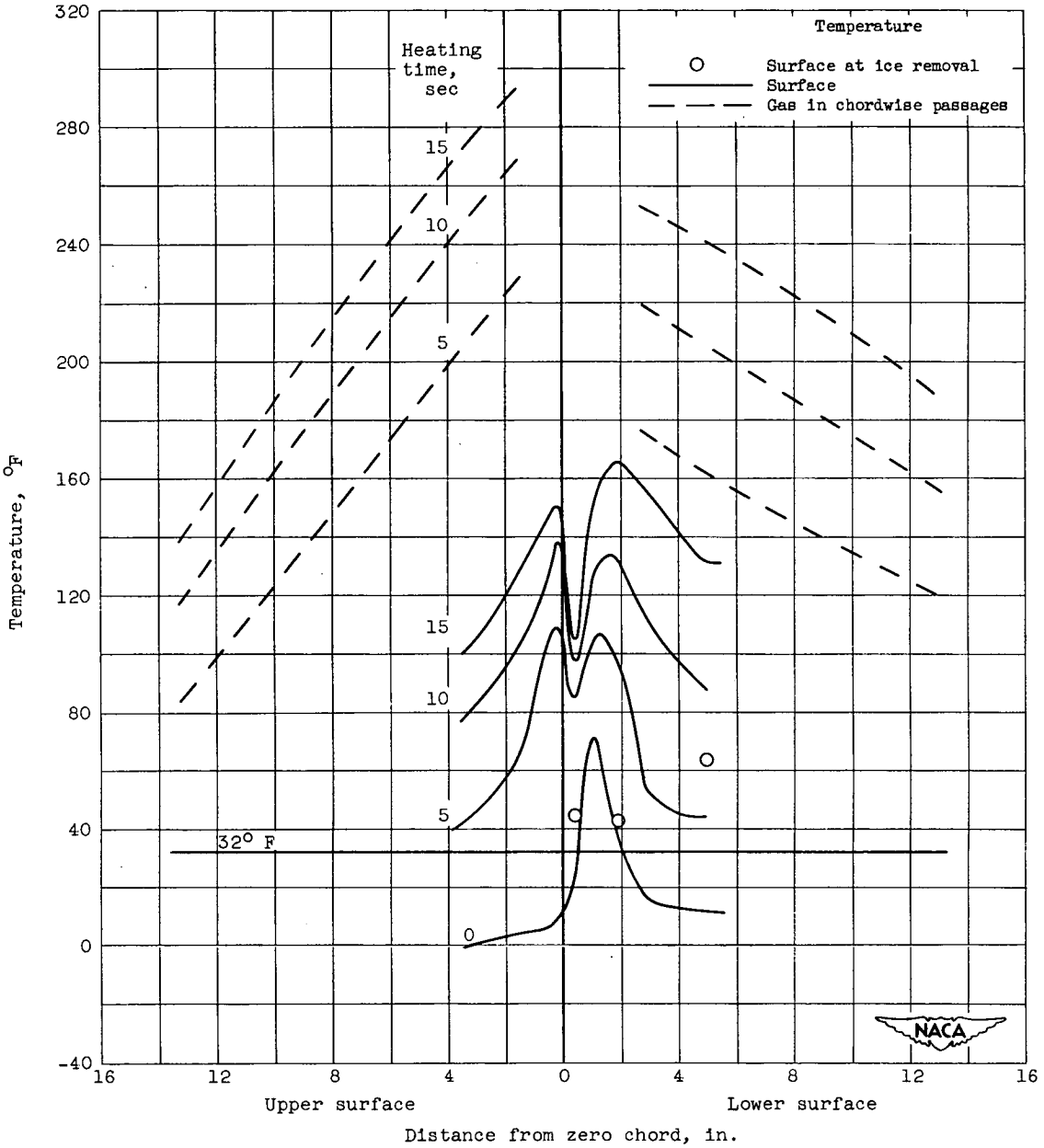

(c) Gas flow, 333 pounds per hour per foot span.

Figure 27. - Concluded. Chordwise variation of surface and gas temperature during heating period with temperature at time of ice removal. Airspeed, 280 miles per hour; datum air temperature, 0° F; liquid-water content, 0.6 gram per cubic meter; angle of attack, 5°; model-inlet gas temperature, 500° F; heating system A.

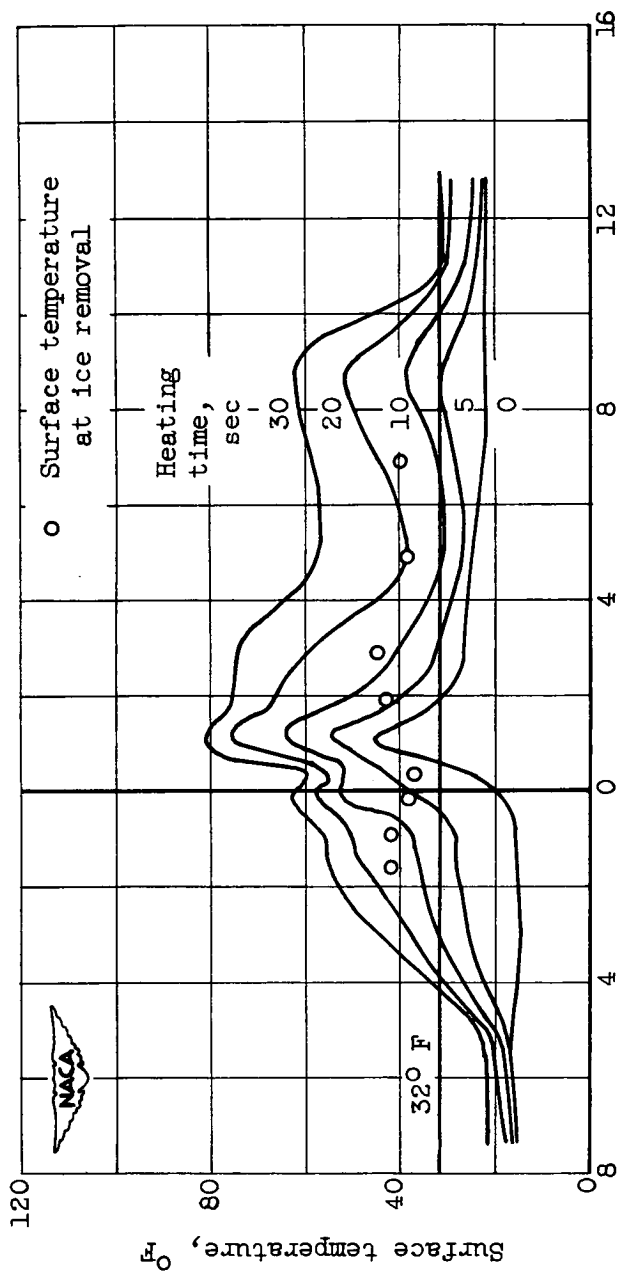

Figure 28. - Chordwise variation of surface temperature during heating period. Airspeed, 280 miles per hour; datum air temperature, 20° F; liquid-water content, 0.8 gram per cubic meter; angle of attack, 5°; gas flow, 167 pounds per hour per foot span; model-inlet gas temperature, 250° F; heating system A.

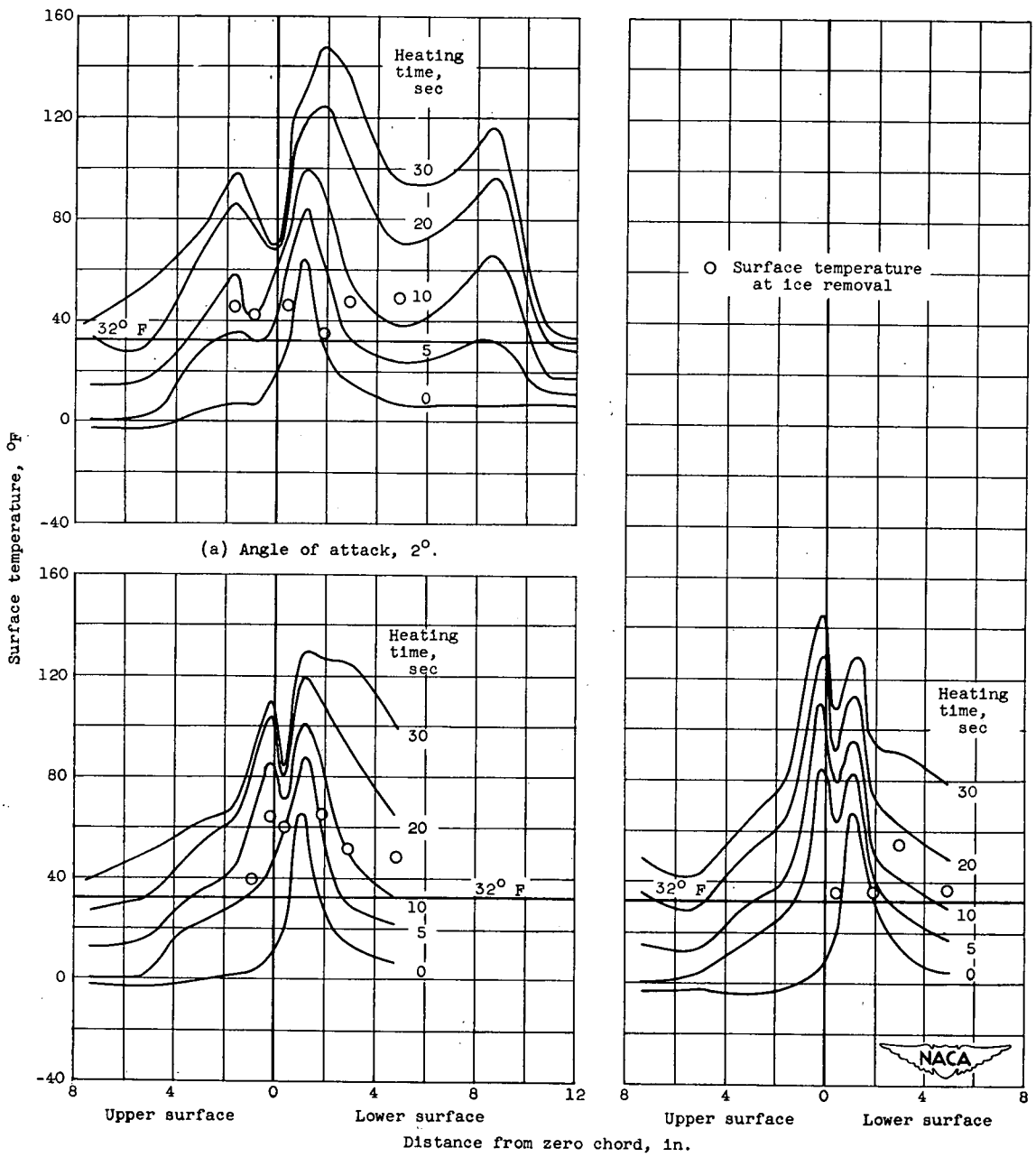

Figure 29. - Effect of angle of attack on chordwise variation of surface temperature during heating period. Airspeed, 280 miles per hour; datum air temperature, 0° F; liquid-water content, 0.6 gram per cubic meter; gas flow, 180 pounds per hour per foot span; model-inlet gas temperature, 500° F; heating system A.

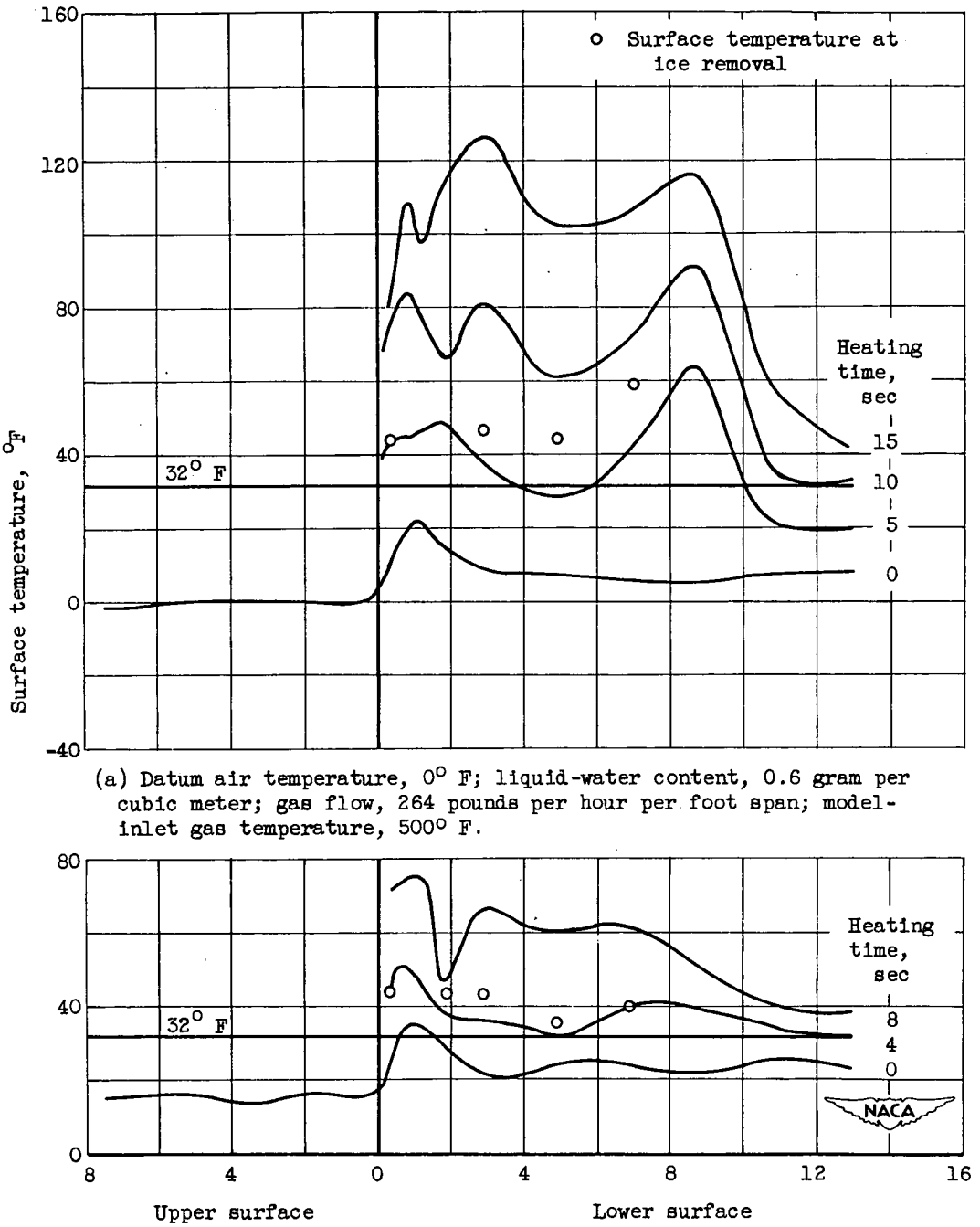

(a) Datum air temperature, 0° F; liquid-water content, 0.6 gram per cubic meter; gas flow, 264 pounds per hour per foot span; model-inlet gas temperature, 500° F.

(b) Datum air temperature, 20° F; liquid-water content, 0.8 gram per cubic meter; gas flow, 370 pounds per hour per foot span; model-inlet gas temperature, 350° F.

Figure 30. - Chordwise variation of surface temperature during heating period of heating system B. Airspeed, 280 miles per hour; angle of attack, 5°.

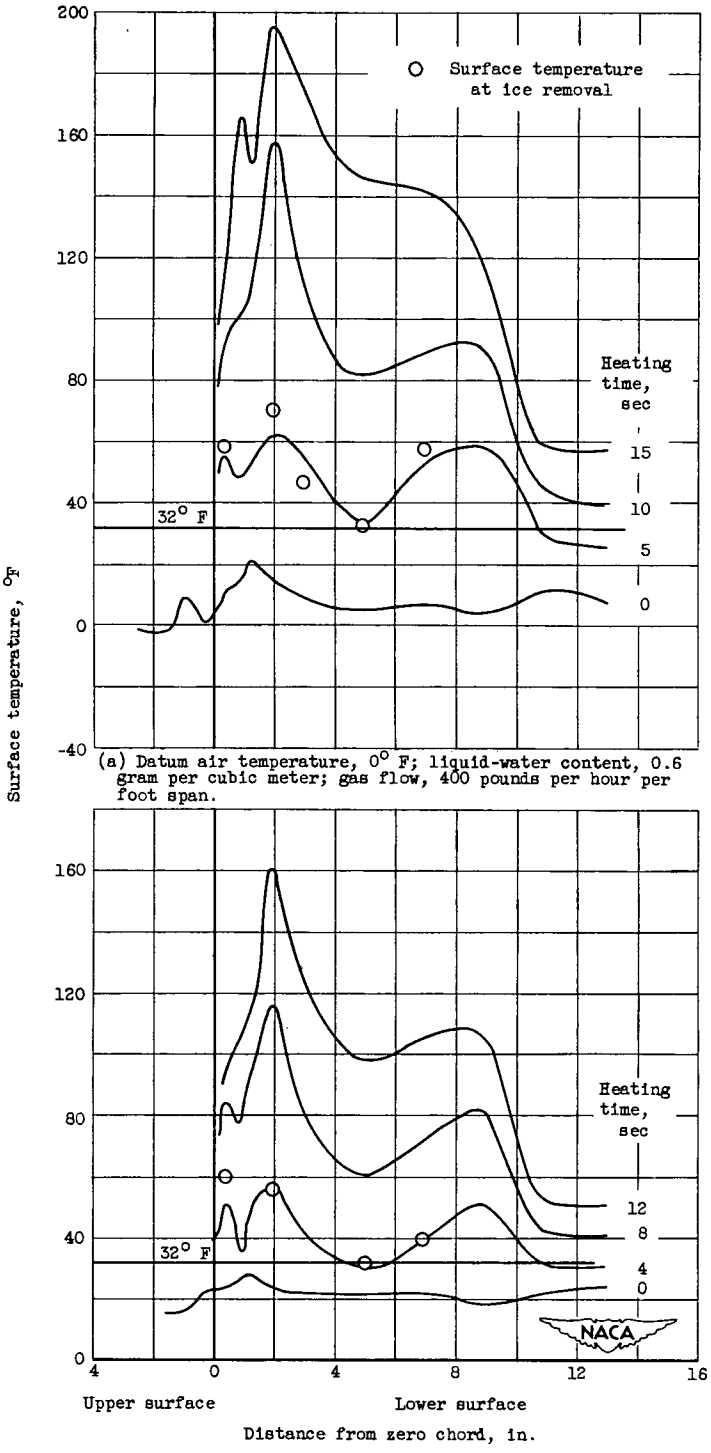

(a) Datum air temperature, 0° F; liquid-water content, 0.6 gram per cubic meter; gas flow, 400 pounds per hour per foot span.

(b) Datum air temperature, 20° F; liquid-water content, 0.8 gram per cubic meter; gas flow, 337 pounds per hour per foot span.

Figure 31. - Chordwise variation of surface temperature during heating period of heating system C. Airspeed, 280 miles per hour; angle of attack, 5°; model-inlet gas temperature, 500° F.

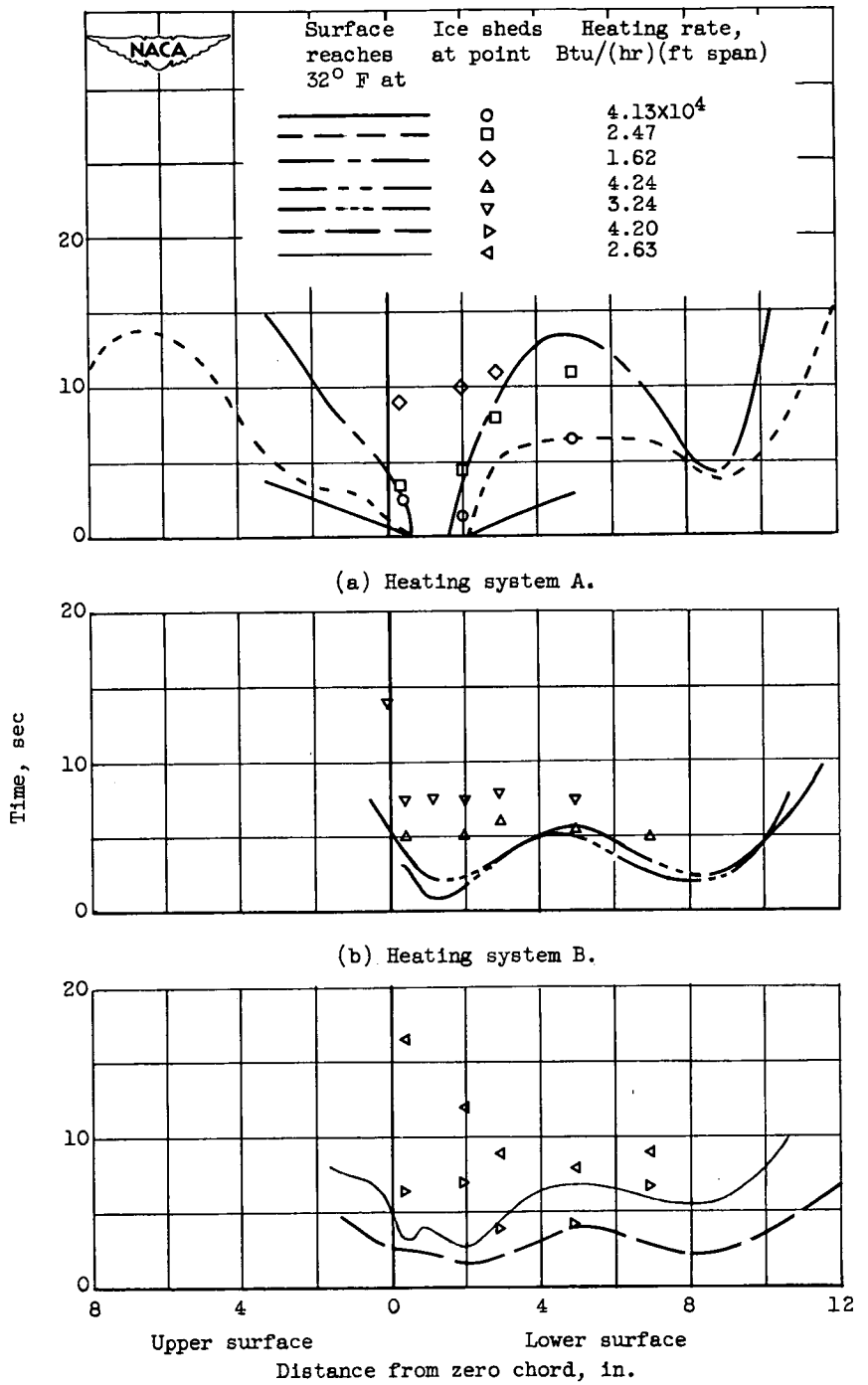

Figure 32. - Chordwise variation of ice-shedding time and time to reach 32° F as a function of heating rate for heating systems A, B, and C. Airspeed, 280 miles per hour; datum air temperature, 0° F; liquid-water content, 0.6 gram per cubic meter; angle of attack, 5°.

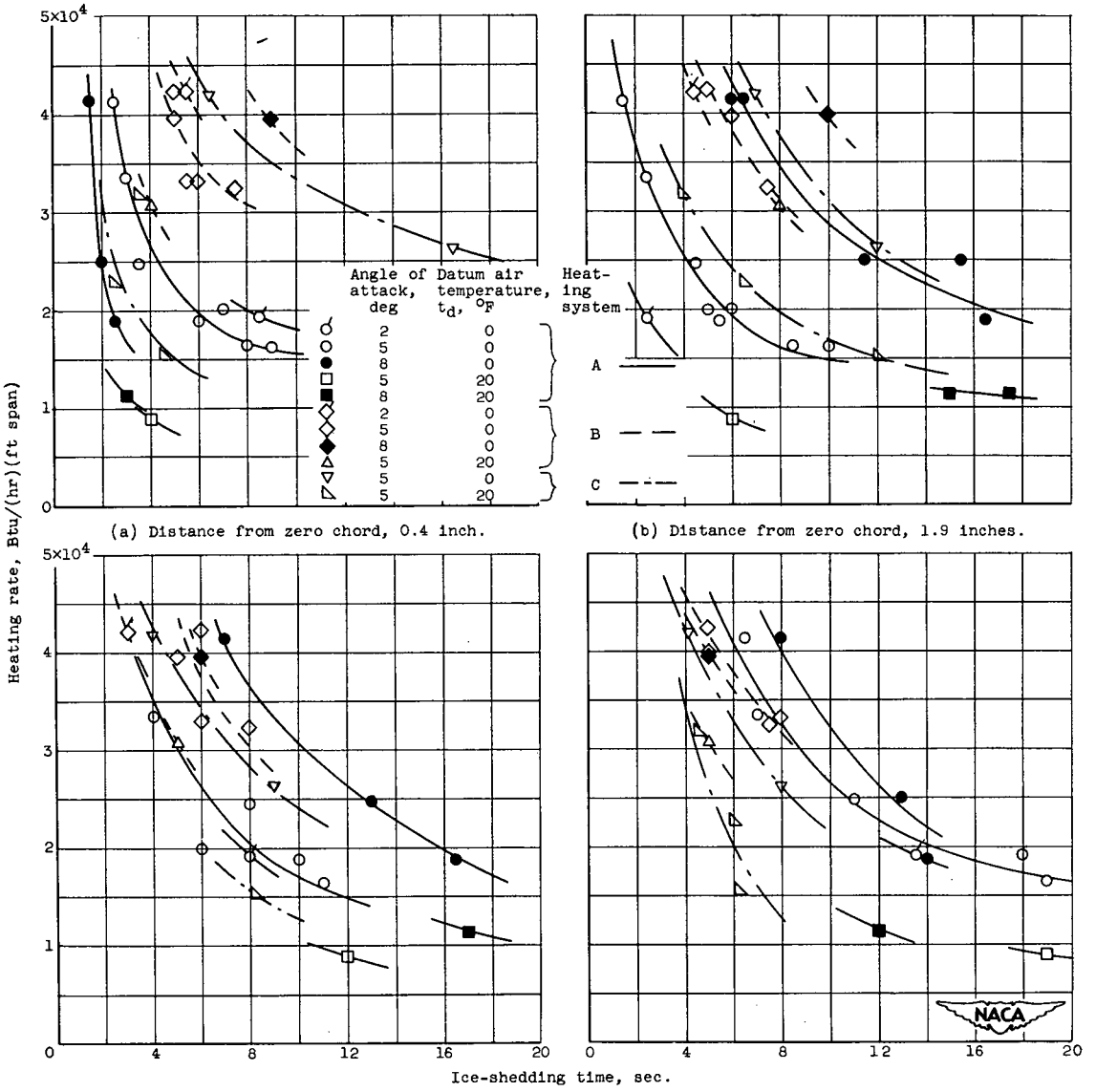

(a) Distance from zero chord, 0.4 inch.

(b) Distance from zero chord, 1.9 inches.

(c) Distance from zero chord, 2.9 inches.

(d) Distance from zero chord, 4.9 inches.

Figure 33. - Ice-shedding time as function of heating rate, angle of attack, datum air temperature, heating system, and lower-surface location. Airspeed, 280 miles per hour; nominal liquid-water content.